School of Finance

University of St.Gallen

MEDIUM-TERM PLANNING FOR THERMAL ELECTRICITY PRODUCTION

RAIMUND M. KOVACEVIC
FLORENTINA PARASCHIV

WORKING PAPERS ON FINANCE NO. 2012/20

INSTITUTE OF OPERATIONS RESEARCH AND COMPUTATIONAL FINANCE
(IOR/CF – HSG)

2012

MEDIUM-TERM PLANNING FOR THERMAL ELECTRICITY PRODUCTION

RAIMUND M. KOVACEVIC FLORENTINA PARASCHIV

Abstract. In the present paper we demonstrate a mid-term planning model for thermal power generation which is based on multistage stochastic optimization and involves stochastic electricity spot prices, mixture of fuels with stochastic prices, the effect of CO2 emission prices and various types of further operating costs. Going from data to decisions, the first goal is to estimate simulation models for various commodity prices. We apply geometric Brownian motions with jumps to model gas, coal, oil and emission allowance (EUA) spot prices. Electricity spot prices are modeled by a regime switching approach which takes into account seasonal effects as well as jumps and spikes. Given the estimated models we simulate scenario paths and then use a novel approach based on a multiperiod generalization of the Wasserstein distance for constructing the stochastic trees used in the optimization model. Finally, we solve a one year planning problem for a fictitious configuration of thermal units, producing against the markets. Numerical examples are used to demonstrate the effect of CO2 prices on cumulated emissions and to show an application of indifference pricing to electricity delivery contracts.

Keywords: multistage stochastic programming, tree generation, electricity production, modeling commodity spot prices

Raimund M. Kovacevic, founded by WWTF, University of Vienna, Dep. of Statistics and Decision Support Systems, Universitätsstraße 5/9 A-1010 Vienna, Austria, T +43-1-4277-38637, e-mail: raimund.kovacevic@univie.ac.at.
Florentina Paraschiv (corresponding author), University of St. Gallen, Institute for Operations Research and Computational Finance, Bodanstrasse 6, CH-9000, St. Gallen, Switzerland, T +41-71-224-3081 e-mail: florentina.paraschiv@unisg.ch.

1. Introduction

Dealing with the stochasticity of commodity and electricity prices is a key issue in contemporary energy markets and cannot be neglected by the producers of electrical power. In this paper we propose a multistage stochastic optimization model for market oriented power production planning. Optimization has a long history in power production planning and in the last years stochastic optimization approaches become more and more important in this field. See e.g. [40],[18], [35], [39] and the overview [42].

In particular, we formulate an optimization model for a thermal system for electricity production. Different types of fuels are bought at fuel spot markets and stored in order to produce electric energy, finally sold at an electricity spot market. Costs involve fuel costs as well as fixed and variable operating costs. In addition we allow for trading at CO2 spot markets in order to have available the necessary amount of emission certificates at the end of the planning horizon. The aim is to maximize the asset value – consisting of a cash position and the value of stored fuel – at the end of the planning horizon. Because the problem is stochastic we maximize a mixture of expectation and average value at risk.

We aim at a simplified model for mid-term planning, that can be used for calculating efficient frontiers, doing some sensitivity analysis or pricing contracts, depending on the contract size[1]. Each step from data to final decisions is described. Finally we implement and solve a concrete one year planning problem for a fictitious configuration of thermal units, optimized against the market prices.

Besides formulating the multistage stochastic optimization problem, which will be done in section 3, this paper also discusses the estimation of the related price models, in particular introducing a regime switching model for electricity spot prices, and uses a novel method for tree construction, recently developed in [24].

Electricity prices have properties that differ considerably from those of other commodities. In particular they show strong seasonalities as well as spiking behavior. While oil, gas, coal and CO2 prices are modeled as geometric Brownian motions with jumps, we estimate electricity spot prices based on the related forward curve and deviations between this curve and actual prices. We estimate these models for european price data and analyze their in- and out of sample performance.

Concrete formulations of the optimization model use the framework of tree-based multistage stochastic optimization. Trees are constructed accordingly to a novel tree approximation method, proposed in [24] and based on the distance concept developed in [32], which uses a multiperiod generalization of the Wasserstein distance as a distance between processes.

Additionally, we bring evidence for two aspects to be considered in the production planning: We implement the proposed approach (for a fictitious but realistic thermal system) and use it to analyze the effects of increasing CO2 prices on the accumulated CO2 emissions. Furthermore, we demonstrate the use of the model to calculate indifference prices for fixed fuel and electricity contracts.

[1]The authors thank Wilfried Grubauer, Willi Kritscha and Walter Reinisch from Siemens AG Austria for interesting discussions about necessary issues, possible simplifications and applications.

The paper is organized as follows: Section 2 gives a short description of the relevant commodity and electricity markets and offers an overview of the price data used later on. In section 3 we develop the basic optimization model. Section 4 then gives a deeper view of the involved risk factors, describes the price models used and the related estimation procedures and analyzes the estimation quality. An overview of tree construction and the tree based reformulation of the optimization model is then given in section 5.1. In the final chapter we describe a concrete numerical example, which is based on approximating trees as described before and use it for case studies on indifference pricing and for some sensitivity analysis of CO2 prices. Finally, in the appendix we give further details of the estimation procedure and the reformulated optimization model, and show further tables and graphics.

2. Data

2.1. **European gas prices.** Within the European Union (EU), a number of mostly smaller market places for natural gas have emerged since the inception of market liberalization (see [41])[2] To avoid working with exchange rate scenarios, we look at one gas price index traded in EUR/MWh[3]: GPL hub, which is operated by Gaspool Balancing Services GmbH. In particular we look at daily GPL spot gas prices provided by Bloomberg, sample period April 2007–December 2011.

2.2. **Oil price data.** Brent Crude is sourced from the North Sea and is a major trading classification of sweet light crude oil comprising Brent Blend, Forties Blend, Oseberg and Ekofisk crudes (also known as the BFOE Quotation). Brent futures on the International Petroleum Exchange help determine prices in the 2 billion-a-day USD world crude oil market and influence the costs of products from gasoline to asphalt. Petroleum production from Europe, Africa and the Middle East flowing West tends to be priced relative to the Brent Crude oil[4]. For our analysis we look at Brent Crude daily spot oil prices, over the sample: May 2003–December 2011 (index EUCRBREN, source Bloomberg).

2.3. **Coal.** Around 30% of the power generated in the EU-27 is coal-based (Euracoal 2011). Europe imports coal mainly from the US and Atlantic market as well as from Africa. Spot coal prices for Europe are published, for example, by McCloskeys key physical prices for North West Europe (NWE) steam coal marker (Index MSCMEUET, source Bloomberg). The McCloskey's Group NWE Market prices are published every week and reflect the actual physical levels of activity. We look at a data sample from 09/12/2005–25/05/2012.

[2]The major gas hubs in the EU are: Natural Balancing Point (NBP) UK, Title Transfer Facility (TTF) Netherlands, Zeebrügge Belgium, NetConnect Germany (NCG), Gaspool (GPL) Germany or Points d'Echange de Gaz (PEG) France.

[3]Comparative statistics of the main European gas prices show no significant differences among them. This is not surprising, since arbitrage should quickly wipe out any temporal differences among them. Results are available under request.

[4]London, July 29 2005 (Bloomberg)

2.4. **CO2 emission allowances.** EU Allowance (EUA) is a permit to emit one metric tonne of CO2 under the European Union Emission Trading Scheme (EU ETS). After April 2006, when the first verified report concerning the actual emissions of each EU member state occurred, prices increased to a maximum level of almost 30 EUR. In the next time, the market participants realized that there was an excess of allocated allowances to the emission intensive firms and, thus, the market was not as short as expected. We assist at a market correction when the EU ETS lost a half of their market value (prices dropped below 5 EUR). For the purpose of our study we avoid the extreme prices drop which occurred in the first trading period (2005–2007) and we look at the second trading period: April 2008 up to December 2011, taking daily observations of EUA spot prices (EUETSSY1 price index provided by Bloomberg).

2.5. **Electricity.** We analyze the electricity prices for the German market. Therefore, we refer to EEX Phelix hourly electricity prices quoted at the European Energy Exchange (EEX), one of the biggest power exchanges in Continental Europe, between September 2008 and December 2011. Electricity delivered on the next day is traded at the day-ahead spot market the. Also futures contracts with a delivery period of one week (since 2011), one month, one quarter or one year are traded at EEX. We construct hourly price forward curves (HPFC) by looking at all traded products. Later on, the HPFC serves us as input for the electricity spot model.

2.6. **Descriptive statistics.** In table D we show descriptive statistics of the gas, coal, oil and EUA prices. The skewness and kurtosis coefficients suggest a leptokurtic distribution with negatively skewed returns in all three investigated markets. This is also confirmed by the Jarque-Bera test results which clearly reject the null hypothesis of a normal distribution for both levels and daily returns. Furthermore, autocorrelations die out slowly in levels, which is consistent with a very persistent, possibly non-stationary variation. To investigate the stationarity properties of the analyzed commodity prices we employ three unit root tests (Table 3). The results suggest that, at conventional significance levels, logarithmic spot prices are non-stationary. This is similar to [10] and it clearly contradicts the common assumption of mean reverting behavior in commodity prices.

3. The Optimization Model

Let in the following $\mathcal{I} = \{1, \dots, I\}$ denote the set of thermal units, $\mathcal{J} = \{1, \dots, J\}$ the set of fuels and $\mathcal{T} = \{\tau_0, \dots, \tau_T\}$ the considered points in time. The producer observes random fuel spot prices $P^f_{t,j}(\omega)$, $t \in \mathcal{T}$, $j \in \mathcal{J}$, random electricity spot prices $P^x_t(\omega)$, $t \in \mathcal{T}$ and random spot prices $P^c_t(\omega)$, $t \in \mathcal{T}$ for CO2 emission certificates. These risk factors are considered as stochastic processes defined on a filtered probability space $(\Omega, (\Sigma_t), \mathbb{P})$. Usually the filtration $\Sigma = (\Sigma_t)_{t=0,\dots,T}$ is modeled as the filtration generated by the random vector $(P^f_{t,cdot}, P^x_t, P^c_t)$, i.e. $\Sigma_t = \sigma\left((P^f_{t,.}, P^x_t, P^c_t), t \in \mathcal{T}\right)$. Decisions will be made regarding the energy $x_{t,i,j}(\omega)$ produced by unit i using fuel j over time period $[\tau_t, \tau_t + \Delta_t]$, where $\Delta_t = \tau_{t+1} - \tau_t$ and the amount of fuel $f_{t,j}(\omega)$ bought from spot market, for all $j \in \mathcal{J}$, $t \in \mathcal{T}$. In our setup it is possible for a generator to use more than one fuel, which means that we are seeking for an optimal fuel mix. Both, $x_{t,i,j}(\omega)$, $f_{t,j}(\omega)$ and c_t are considered as

Σ_t-measurable, which means that decisions have to be taken based on information available at time t.

In the following most equations and inequalities contain indices $i \in I$, $j \in J$ or $t \in \{0, 1, \ldots, T\}$. If no special assumption is stated, it is assumed that they hold for all values of any occurence of such an index.

It is not possible to produce negative amounts of energy, and we do not allow for selling back fuel, which leads to the following restrictions:

$$x_{t,i,j} \geq 0, \quad f_{t,j} \geq 0. \tag{3.1}$$

In practice amounts of fuels are measured by a huge variety of units, depending on both markets and the particular fuel. To avoid the usage of conversion factors in the notation as much as possible, all amounts of fuel are expressed by their energy content , i.e. they have been converted to MWh. As a consequence all fuel prices are expressed in EUR/MWh. To be consistent, electric energy is measured in MWh too and its price is given in EUR/MWh. In addition, $c_t(\omega)$ will denote the amount bought (if positive) or sold at the CO2 emission market. CO2 emissions and the amounts of certificates traded are expressed in (metric) tons and hence the certificate price in $EUR/tonne$. We will express all random variables without explicitly referring to the elements $\omega \in \Omega$ of the state space in the following. Because electricity is produced and simultaneously sold over periods $[\tau_t, \tau_{t+1}]$ the prices P_t^x have to be interpreted as weighted mean prices achieved over the whole period. The same holds true for the other random prices.

3.1. **Thermal power plants, fuels and the basic cost model.** Different types of power plants are characterized by their efficiencies for different fuels, the maximum power produced and the cost structure, which together defines the merit order of turbines in the system. In the simplest setup each thermal generator i is characterized by efficiencies $\eta_{i,j}$ for producing electric energy with fuel j and the maximum power β_i (in MW) that can be produced. In particular the produced energy is restricted by

$$\sum_{j=1}^{J} x_{t,i,j} \leq \beta_i \cdot \Delta_t. \tag{3.2}$$

Three kinds of cost are used throughout this paper: fuel costs, variable and fixed operating costs. In addition interest has to be paid for borrowing money. The fuel used for producing an amount of energy $x_{t,i,j}$ is given by $x_{t,i,j}/\eta_{i,j}$, hence the related fuel costs are given by $P^f_{t+1,j}(\omega) \cdot x_{t,i,j}/\eta_{i,j}$. It is assumed that the fuel price is known only after deciding about the amount of fuel used. The variable operating costs c_i (in EUR/h) depend on the effective amount of time a machine is used and includes, e.g., variable personnel costs and maintenance costs. The usage time is estimated by $x_{t,i,j}/\beta_i$. Finally, we include fixed operating costs, including personal as well as maintenance and capital costs. At first glance it might seem that fixed costs do not influence the optimal solution. However, we assume that fixed costs have to be paid at each decision period and we will distinguish between positive and negative amounts of cash. Because interest paid on a negative cash position

(debt) is usually higher than interest on positive cash, fixed costs have an effect on the risk of the decision problem.

Because in our examples, we aim at mid-term planning with weekly decisions, we will not use switching, ramping, or minimum power production constraints. Such constraints are most relevant in hourly (or daily) decision models and lead to mixed integer models. While comparably efficient formulations exist for deterministic planning (see e.g. [11] or [8]), it is very difficult to include mixed integer constraints in a large stochastic problem, especially if calculation time is critical. As an example see, e.g., [30]. We are also avoiding efficiencies that depend on the power produced. By avoiding such complications it is possible to enhance the complexity of the stochastic model, and finally to use more scenarios.

3.2. **Storage, CO2 and cash accounting.** In the following we introduce storages $s_{t,j}$ for each fuel j, cumulated CO2 emissions e_t, cumulated CO2 certificates a_t and a cash position w_t. These decision variables are stochastic processes, adapted to the filtration Σ. With initial storage amounts s_j^0 and maximum storage amounts $\bar{s}_j$ each storage develops according to

$$s_{0,j} = s_j^0, \quad s_{t,j} = s_{t-1,j} + f_{t,j} - \sum_{i=1}^{I} \frac{x_{t-1,i,j}}{\eta_{i,j}} \qquad \forall t > 0, j \tag{3.3}$$

$$0 \le s_{t,j} \le \bar{s}_j \qquad \forall t, j. \tag{3.4}$$

Note that equation (3.3) models storage as the amount stored immediately before the beginning of the next production period $(\tau_t, \tau_{t+1}]$. It is assumed that fuels are bought and stored at times τ_t, while they are used for electricity production over periods $(\tau_t, \tau_{t+1}]$.

The production during any period $(\tau_t, \tau_{t+1}]$ is restricted by

$$\sum_{i=1}^{I} \frac{x_{t,i,j}}{\eta_{i,j}} \le s_{t,j} \qquad \forall t, j. \tag{3.5}$$

Storage costs are based on a cost factor ζ_j (EUR/MWH/h) for each fuel and are averaged for each time period, see 3.11.

CO2 emissions and the related costs are modeled in the following way: At the beginning the amount e^0 of CO2 emitted before the planning horizon is known and during each period emissions e_t accumulate as follows:

$$e_0 = e^0, \quad e_t = e_{t-1} + \sum_{j=1}^{J} \sum_{i=1}^{I} \frac{\varepsilon_{ij}}{\eta_{i,j}} \cdot x_{t-1,i,j} \qquad \forall t > 0. \tag{3.6}$$

Here ε_{ij} denotes the amount of emissions (in metric tons, t) per MWh of energy produced by unit i with fuel j. At each time it is possible to buy ($c_t > 0$) or sell ($c_t < 0$) certificates at the market for CO2 allowances at prices P_t^c. Again, we start with a known amount a^0 of certificates bought before the beginning and describe the certificate-position by

$$a_0 = a^0, \quad a_t = a_{t-1} + c_t \qquad \forall t > 0. \tag{3.7}$$

Clearly the emission accounts have to be restricted by

$$a_t \geq 0, \quad e_t \geq 0, \quad \forall t \geq 0. \tag{3.8}$$

As we will see, a penalty, payable at the end of the planning horizon, ensures that emissions do not exceed the certificates hold.

Given all cash flows from fuel usage, storage, CO2 emissions and certificates we are able to define accounting equations for the cash position. At time $t = 0$ we start with

$$w_0 = w^0 - \sum_{j=1}^{J} P^f_{0,j} f_{0,j}. \tag{3.9}$$

For $0 < t < T$ it is necessary to account for interest, fuel costs, cash flows from selling the produced electricity and from trading with certificates, storage costs and finally for operating costs. In order to deal with interest rates and debt, the cash position is splitted into a positive and a negative part, w_t^+, w_t^- which allows to apply different interest rates for borrowing ($w_t^- > 0$) and lending ($w_t^+ > 0$):

$$w_t = w_t^+ - w_t^-, \quad w_t^+ \geq 0 \quad w_t^- \geq 0 \qquad \forall t > 0. \tag{3.10}$$

We use interest rates ρ_b for borrowing and ρ_l for lending such that $\rho_b > \rho_l$.Because of the difference between the two interest rates it is possible to avoid the explicit complementarity restrictions $w_t^+ \cdot w_t^- = 0$. Finally, with ζ_j denoting storage costs for fuel j per time unit, γ_i (EUR/h) denoting variable operating costs of generating unit i per time unit and κ_i (EUR/h) denoting fixed operating costs of generating unit i per time unit the cash position updates in the following way:

$$\begin{aligned}
w_t &= (1+\rho_l) w_{t-1}^+ - (1+\rho_b) w_{t-1}^- && \text{(3.11a)}\\
&- \sum_{j=1}^{J} P^f_{t,j} \sum_{i=1}^{I} f_{t,j} - P^c_t c_t && \text{(3.11b)}\\
&+ P^x_t \cdot \sum_{i=1}^{I} \sum_{j=1}^{J} x_{t-1,i,j} && \text{(3.11c)}\\
&- \sum_{j=1}^{J} \zeta_j \frac{(s_{t,j} + s_{t-1,j})}{2} \Delta_{t-1} && \text{(3.11d)}\\
&- \sum_{i=1}^{I} \frac{\gamma_i}{\beta_i} \cdot \sum_{j=1}^{J} x_{t-1,i,j} - \kappa_i \cdot \Delta_{t-1} \quad 0 < t < T && \text{(3.11e)}
\end{aligned}$$

At time T no fuel is bought anymore, but the certificates have to be cleared: The difference between current cumulated emissions and the amount of emissions covered by the certificates held is valued at the actual certificate price plus $\theta = 100$ EUR/t penalty and the resulting amount has to be paid from cash. For simplicity we assume here that the settlement of certificates is done at

the end of the planning horizon. Hence the cash position at time T is given by

$$
\begin{aligned}
w_T &= (1+\rho_l)w^+_{T-1} - (1+\rho_b)w^-_{T-1} \\
&+ P^x_T \cdot \sum_{i=1}^{I}\sum_{j=1}^{J} x_{T-1,i,j} \\
&- \sum_{j=1}^{J} \zeta_j \frac{(s_{T,j}+s_{T-1,j})}{2}\Delta_{t-1} \\
&- \sum_{i=1}^{I} \frac{\gamma_i}{\beta_i} \cdot \sum_{j=1}^{J} x_{T-1,i,j} - \kappa_i \cdot \Delta_{T-1} \\
&- (\theta + P^c_T)(e_T - a_T)^+.
\end{aligned} \tag{3.12}
$$

3.3. **The objective function and the overall optimization problem.** The producer aims at maximizing the revenue over the planning horizon. We base the decision on the sum of the cash position, the value of stored fuels at market prices – the *asset value* v_T – at the end of the planning horizon.

$$
v_T = w_T + \sum_{j=1}^{J} s_{T,j} \cdot P^f_{T,j} + (a_T - e_T)^+ \cdot P^c_T. \tag{3.13}
$$

It is assumed that selling of certificates is not possible anymore at time T. Because v_T is a random variable we use a mixture of expectation and average value at risk as the objective. The average value at risk is defined as

$$
AV@R_\alpha(X) = \int_0^\alpha F^{-1}(p) \tag{3.14}
$$

for a random variable X with c.d.f. F. See [15, 33] for more details on $AV@R$ and the related class of polyhedral risk and acceptability measures and [14] for further applications in electricity production.

With a weighting factor $0 \le \lambda \le 1$ we write the generators decision problem as

$$
\begin{aligned}
\max_{x,f,c,(s,w,v,a,e)} \quad & \lambda \cdot \mathbb{E}\left[v_T\right] + (1-\lambda) \cdot AV@R_\alpha(v_T) \\
s.t. \quad & (3.1) - (3.13) \\
& x, f, c \triangleleft \Sigma \\
& s, w, v, a, e \triangleleft \Sigma
\end{aligned} \tag{3.15}
$$

where the last constraints demand that all decision variables are adapted to the filtration Σ.

4. Price models

We aim at an optimization problem with 5 driving random factors (gas, coal, oil, CO2 and electrictiy prices). The first question in estimating the related price models is, whether it worthwile to estimate a joint model. While it seems reasonable that some dependencies between those markets

might be relevant, the literature on joint models for commodity prices is scarce. However, we can mention in this sense [31], which propose a multi-factor model for the joint dynamics of related commodity spot prices in continuous time, with an application on crude/heating oil and gasoline prices. Another example is [36], who derive a hybrid commodity and interest rate market model. However, the study refers mainly to futures commodity markets and with application to oil prices. [29] shows how to build a stochastic model for commodity price behavior that matches the current term structure of forward and futures prices. [9] found that long-term co-movement among commodities is driven by economic relations, as an application for oil prices. However, all these cited models are applied to oil/gasoline prices. To our knowledge, a joint model tested simultaneously for different European commodity prices (gas, oil, coal etc.) was not published so far.

As a starting point we investigated whether there are significant co-movements in the commodity prices described in section 2 in such a way that a joint simulation model can be derived. Thus, we applied Principal Component Analysis (PCA) to see whether there are joint factors driving the commodity prices. For this purpose, we looked at daily data between April 2008 up to December 2011 for gas, (crude) oil, CO2 emission allowances and electricity prices as described in the previous section. The coal prices were left apart, since we have available only weekly observations in this case. Generally spoken, we observe very low correlations (see table 4). There is some correlation (< 0.2) between CO2 emission rights and oil prices, between CO2 and gas (< 0.1) as well as between gas and electricity (< 0.1). The PCA shows that the first factor explains 31%, the first two factors explain 58% of the variance, etc. The eigenvalues of all four factors are relatively close, so we cannot conclude clearly that there are factors which explain most of the variation of all included prices (see table 5). The rotated component matrix also shows that basically each factor drives one commodity (see table 7). Thus, there is no clear evidence for motivating the use of a joint factor model for all prices. Furthermore, we performed a cointegration analysis pairwise and including all prices at once in the analysis, but did not get conclusive results.[5]

4.1. **Modeling commodity prices: gas, oil, CO2 and coal prices.**

4.1.1. ***Overall Approach.*** The descriptive statistics of gas, oil and EUA spot prices indicate that the energy spot prices are likely to be characterized by non-stationarity and jumps, as indicated by the skewness and kurtosis of the investigated prices. A model based on the standard Brownian motion process assumptions would be too limited in this case. We therefore apply the jump-diffusion model of [28] – Geometric Brownian motion augmented by jumps (GBMPJ) – which, accordingly to literature (e.g., [28], [38], [4] or [27]), shows a good performance in modeling the dynamics of commodity prices. In a recent study of the three main markets for emission allowances under the EU ETS, [10] show that spot prices are best approximated by a Geometric Brownian motion augmented by jumps. Studies which focus on oil price models (see [38], [27]) discuss also typical effects like mean reversion, structural breaks and jumps. They conclude that Geometric Brownian motion is not appropriate as a long term model because of time varying volatility. The returns may even exhibit

[5]Results are available on request.

many jumps of a magnitude completely inconsistent with a Gaussian density function. Furthermore, inclusion of mean reversion led to deterioration in the accuracy of density forecasting. The studies show that oil prices can be modeled as a jump-diffusion process with time varying volatility and no mean reversion. Our investigated data sample includes periods of significant and sudden large oil price movements including the market stress caused by the invasion of Iraq in 2003, and the recent financial crisis, starting 2008. However, recent empirical studies conclude that it is fruitless to model oil prices by considering specific events in detail. Thus, [27] conclude that structural breaks that occur in the oil market are too frequent to model and that modeling individual structural breaks does not improve the out of sample forecasting accuracy. Therefore, we will focus on modeling jumps and not on the individual causing events.

Concerning gas prices, [26] and [41] employ PCA and show that a two-factor model is expected to be sufficient in replicating the dynamics of futures contracts. One-factor vs. two-factor models are tested, both implying a mean-reverting spot price. The two-factor model performs significantly better in explaining gas prices due to the incorporation of the mean reversion effect in the first risk factor. However, as discussed previously, in the case of the CO2 and oil prices mean reversion models underperformed the GBMPJ. Our purpose is to select a more general pricing model which describes the common statistical properties identified for our considered energy prices and therefore we have chosen the latter.

We estimate the Merton model following the discussion in [20]. The occurrences of Jumps are modeled as Poisson process with $dJ_t \sim Po(\lambda dt)$, and the jump amplitude Y_t is assumed to be log-normally distributed, i.e., $\log(1+Y_t) \sim N(\mu, \delta^2)$. Thus, the log spot price has the form:

$$\log(S_t) = \log(S_0) + (\alpha - \frac{1}{2}\sigma^2)t + \sigma W_t + \sum_{0<s\leq t} \log(1 + Y_s dJ_s). \tag{4.1}$$

Details about the maximum likelihood estimation procedure are offered in the Appendix.

4.1.2. ***Results***. Our parameter estimates for gas, oil, coal and EUA prices are summarized in table 8. For a robustness check we also perform an out-of-sample test by reestimating the parameters for a shorter sample which ends on 1st Dec. 2010. It shows that the estimated parameters are not sample dependent. The jump intensity λ has the largest value in the case of the gas prices. Oil prices show the lowest jump intensity estimates. This is consistent with the kurtosis, skewness and Jarque-Bera values which are the largest in case of gas (and the smallest for oil), as shown in table D.

Figures D.2, D.3, D.4 and D.5 show the means and quantiles of 1000 scenarios simulated for oil, EUA, gas and coal spot prices based in the GBMJ model starting in 1st December 2011 for a horizon of 300 days and compares it with the evolution of the real prices in the subsequent time period. One can see that the scenario means reflect the spot price dynamics in a realistic way for all commodities.

4.2. **Modeling electricity prices.**

4.2.1. ***Preliminaries***. Electricity prices have properties that differ considerably from those of other financial assets or even of other commodities (see [21], [5]). Therefore, we treat them separately. The seasonal – yearly and weekly – behavior of the electricity prices is one of the most complicated

ones among all commodities. It is predominantly caused by the almost inelastic short-term demand for electricity, which by itself shows pronounced patterns caused by economic and business activities. Combined with the lack of efficient storing opportunities for electricity, which prevents intertemporal smoothing of the demand by holding storages, extremely large price movements (spikes) as well as various cyclical patterns of behavior occur. Beside this, the capacity to store electricity is very limited and it is expensive or even damaging to change the production of big generating units, which are further causes for spikes and even negative electricity prices. From an economic perspective, negative prices can be rational, e.g., if the costs to shut down and ramp up a power plant unit exceed the loss for accepting negative prices (see [21]). Since 1st September 2008, negative price bids are allowed at the German power exchange EEX, as the first energy exchange in Europe. Historical spot market data over the investigated period show a total amount of about 100 hours with negative prices. Mostly, they occur during the night and early morning hours (23:00 to 08:00) as displayed in Figure D.6.

The load as one main driver of electricity prices shows some noticeable patterns such as the peak at midday in summer days. On the other hand electricity prices follow more or less typical seasonal patterns, which are usually modeled by deterministic functions. However, as discussed in [21], beside the deterministic impact factors, electricity spot prices are also influenced by uncertain parameters like power plant outages and fluctuant renewable electricity generation. These uncertainties are drivers of the stochastic component of the spot prices. Thus, we base our modeling approach on seasonalities as deterministic components of electricity prices, as well as on the market expectation by using an hourly price forward curve. Subsequently, we apply a regime switching model, reflects big fluctuations of the market spot price around the hourly price forward curve: Upward and downward spikes may occur with a certain probability.

4.2.2. ***Construction of the hourly price forward curves.*** For the derivation of the HPFCs we follow the approach introduced by [16]. At any given time the observed term structure at EEX is based only a limited number of futures/forward products. Hence, a theoretical hourly price curve, representing futures for individual hours, is very useful but must be constructed using additional information. We model the hourly price curve by combining the information contained in the observed bid and ask prices with information about the shape of the seasonal variation.

Let f_t be the price of the forward contract with delivery at time t, where time is measured in hours, and let $F(T_1, T_2)$ be the price of forward contract with delivery in the interval $[T_1, T_2]$. Since only bid/ask prices can be observed, we have:

$$F(T_1,T_2)_{bid} \leq \frac{1}{\sum_{t=T_1}^{T_2} \exp(-rt/a)} \sum_{t=T_1}^{T_2} \exp(-rt/a) f_t \leq F(T_1,T_2)_{ask} \tag{4.2}$$

where r is the continuously compounded rate for discounting per annum and a is the number of hours per year. A realistic price forward curve should capture information about the hourly seasonality pattern of electricity prices. For the derivation of the seasonality shape of electricity prices we follow [5] (chapter 6). A summary of this procedure is offered in the Appendix; Basically we fit the HPFC

to the seasonality shape by minimizing:

$$\min \left[\sum_{t=1}^{T} (f_t - s_t)^2 \right] \tag{4.3}$$

subject to constraints of the type of equation (4.2) for all observed instruments. f_t is the HPFC at time t and s_t is the seasonality curve at hour t (see derivation in the Appendix).[6] For details see [16]. To keep the optimization problem feasible overlapping contracts, as well as contracts with delivery periods which are completely overlapped by other contracts with shorter delivery periods, are removed.

4.2.3. ***Regime switching model for electricity prices***. An important characteristic of electricity prices are their spiking behavior, also called "jump groups" (see [21]): Prices jump into another price level called "spike regime" and afterwards jump back to the base price level, called "base regime". Therefore regime-switching approaches for electricity prices are often employed in literature (see for example [21]).

We calibrate our model using HPFC generated for the next trading day at EEX (first day HPFC), but also consider the fluctuation of spot prices around the HPFC, due to risk factors such as power plant outages, fluctuant renewable electricity generation etc. Since the prices on the spot market vary in general for each hour of the day, probabilities for upwards or downwards spikes are derived for each hour of each week day (168 parameters). The probability values quantify the likelihood that the spot price is in the Gaussian or "base regime" or in one of the upper or lower spike regimes. Furthermore, we assume that upward or downward spikes are exponentially distributed and we determine the expected spike size for each hour of each week day.

The model can be described by

$$MCP_t = \begin{cases} f_t^L - Spike_t^- & \text{with } p_h^- \\ f_t \cdot \exp(r_t) & \text{with } 1 - p_h^- - p_h^+ \\ f_t^U + Spike_t^+ & \text{with } p_h^+ \end{cases}$$

with

$$\begin{aligned} Spike_t^+ &\sim \text{Exp}(\lambda_h^+) \\ Spike_t^- &\sim \text{Exp}(\lambda_h^-) \\ r_t &\sim N(0, \sigma_h^2) \\ f_t^L &= f_t * \exp(-\alpha_h) \\ f_t^U &= f_t * \exp(\alpha_h) \end{aligned}$$

where:

[6] In the original model [16], applied for daily steps, a smoothing factor prevents large jumps in the forward curve. However, in the case of hourly price forward curves, [5] (pp. 154) concludes that the higher the relative weight of the smoothing part, the more the hourly structure disappears. We want that our HPFC reflects the hourly pattern of electricity prices and therefore in this study we set the smoothing term to 0.

MCP_t**:** Market clearing price (or spot price) for time t measured in hours
f_t**:** HPFC, forward price for hour t
h**:** Index of the week hour that corresponds to time t, i.e., $h(t) : t \to \{1, \ldots, 168\}$
$Spike_t^+$**:** Spike (upwards) exponentially distributed with parameter λ_h^+
$Spike_t^-$**:** Spike (downwards) exponentially distributed with parameter λ_h^-
f_t^U**:** Upper limit of the Gauss dynamics
f_t^L**:** Lower limit of the Gauss dynamics
r_t**:** Normally distributed random variable $N(0, \sigma_h^2)$

Parameter list:

p_h^+**:** Probability for spike upwards
p_h^-**:** Probability for spike downward
σ_h**:** Volatility of the Gaussian dynamics
λ_h^+**:** Parameter of the exponential distribution for upward spikes
λ_h^-**:** Parameter of the exponential distribution for downward spikes
α_h**:** Delimitates the upper/lower bounds of the "base regime"

The model parameters are estimated using a maximum likelihood estimation procedure, see Appendix C for details.

4.2.4. ***Results.*** Our estimation results for each hour of week day are presented in tables 10 and 11. The expected values for each hour of the upward or downward spikes, $1/\lambda_h^+$ and $1/(-\lambda_h^-)$ are given in EUR/MWh. We observe that large spikes are expected to occur during the night hours, as well as during the midday and evening peak hours. Furthermore, we have a higher volatility σ_h^2 during the midday and evening peak hours. Probabilities per hour for spikes upward or downward, p_h^+ and p_h^- are given in %. There is a larger probability that electricity prices fall into the lower "spike regime" during the night hours. This result is in line with our findings from figure D.6. For each day hour, there is a higher probability that large spikes occur during Sundays, which is also confirmed by the literature (see for example [21]). The parameter α_h was estimated at 1.6 standard deviations. It means that the spot prices in the spikes regimes are more than 1.6 standard deviations away from the HPFC.

After calibrating the model, several simulations were carried out to evaluate the goodness of fit in and out of sample. Figure D.8 summarizes the quantiles over 1000 scenarios for the spot electricity prices, for a horizon of one month, starting in September 2008 (for an in sample test) and in December 2011 (out of sample). We observe that the simulated electricity spot prices reflect the *daily, weekly and annual cycles* of electricity prices. Furthermore, the model generates important properties like *single peaks* or *jump groups* and the *mean reverting property* is captured very well by the model.

From the graphical comparison of simulated and historical prices, it can be concluded that the simulated electricity price curve is similar to the observed one. In addition different quality factors

such as the R^2 and the mean average percentage error (MAPE)[7] are computed for different estimation samples. Table 9 summarizes the results. The statistics show that the model performance is not sample dependent.

5. Reformulation as a multistage stochastic optimization Problem

Problem 3.16 cannot be solved directly. In order to solve concrete instances within the framework of multistage stochastic optimization it has to be reformulated on a discrete probability space: the process oriented formulation 3.16 is replaced by a tree oriented formulation in the following. In particular we describe the construction of reasonable trees from estimated models, using a method developed in [24], which is based on a novel distance concept, recently introduced in [32].

5.1. **Reformulation on a tree.**

Consider now a finite probability space $\Omega = (\omega_1, \ldots, \omega_k)$ with K scenarios. Any stochastic process defined on this sample space can be represented as a finite tree with node set $\mathcal{N} = \{1, \ldots, N\}$, where node 1 represents the root.

The levels of the tree correspond to the decision stages. Let $\mathcal{N}_t$ be the set of nodes at level t, for $t = 0, \ldots, T$. The last level $\mathcal{N}_T$ contains the K leaves of the tree which represent the scenarios: $\mathcal{N}_T = \Omega = (\omega_1, \ldots, \omega_K)$. The tree structure (related to the filtration of the process) can be defined by stating the predecessor node n_- for each node n. The set of child nodes is denoted by n_+. There is a unique root node, by convention denoted with 0, which represents the present. Furthermore, each node n carries a probability $Q_n \geq 0$ with $\sum_{j \in \mathcal{N}_t} Q_j = 1$ for all points in time t. By construction there is a one to one relation between any node n and an assigned pair (ω, t), which means that each node is related to the state of the system at time t in scenario ω and vice versa.

We use trees to represent the filtration: Basically those trees carry the price processes P^x, P^f, P^c, i.e. prices P^x_n, P^f_n, P^c_n are associated to each node n. Moreover the decision variables x, f, c, s, w, v, a, e are also related to the nodes which ensures measurability. This leads to a modified notation. So far $x_{t,i,j}$ denoted the random vector of produced energy in period $[t, t+1]$. From now on (in discretized models) $x_{n,i,j}$ will denote the value of produced energy planned at node n and produced in the time period between n and its successor nodes.

Furthermore, the almost sure constraints are defined by formulating them for all (relevant) nodes and the objective function bases on the probabilities related to the nodes: The expectation is directly calculated by weighting the values at each leaf node with the respective probability. For the $AV@R$ it is well known (see, e.g., [37]) that it can be rewritten as

$$\mathbb{AV@R}_\alpha(W) = \max\left\{ g - \frac{1}{\alpha}\mathbb{E}\left[W - a\right]^- : g \in \mathbb{R} \right\}, \tag{5.1}$$

which can be used to reformulate the restriction $\mathbb{AV@R}_\alpha(W) \geq q$ in the following way:

$$\exists a \geq q, \exists Z \geq 0 \text{ such that } W - g + Z \geq 0 \text{ and } q \leq g - \frac{1}{\alpha}\mathbb{E}(Z). \tag{5.2}$$

[7]The MAPE represents the normalized deviation of simulated prices from historical ones in absolute numbers (see [21], p. 12)

This reformulation will be used for a epigraphical representation of the $AV@R$-part of our objective function.

Given the tree-structure defined by the predecessor relation, the above notation, and using the constraints (5.2) for reformulating the objective function the discrete version of the optimization problem (3.15) can be stated easily: Figure (D.1) shows the full formulation.

Thanks to the simplifying assumptions this is an LP. It should be noted that typically the used trees are not very dense: If the time horizon is one year and the decision periods have a length of one week a binary tree would lead to a number of nodes around $9 \cdot 10^{15}$. While for LPs without integer variables it is easily possible to solve instances with several millions variables and constraints, even binary trees will lead to instances that cannot be calculated anymore. In reality, the trees will be sparse: most of the paths in the tree will not have any branches most of the time.

Note that in our model it is possible to buy and sell emission certificates. This can lead to unbounded solutions (arbitrage opportunities) because predictability is high for sparse trees. In order to avoid this difficulty, we will allow trading of emission certificates only in nodes with more than one successor: Therefore we introduce the constraints

$$n \in \mathcal{N}^b_{\neg 0} : \quad a_n = a_{n_-} + c_n,$$

where $\mathcal{N}^b$ denotes the set of nodes with more than one successor, see figure D.1.

5.2. **Tree construction.** Starting from an estimated model for the relevant prices we construct a big scenario tree (with, e.g., several thousand leaf nodes) with given tree structure. A straightforward method consists in simulating random values for all nodes in the tree. As an alternative one might first simulate many scenario paths which are then reduced to a big tree by some tree reduction method, see, e.g., [13] or [19]. For reasonable planning problems with decision periods representing the hours of a day or the weeks of an year even the big tree will not branch at each node. In a second step the big tree is reduced to a smaller tree, which is finally used as the basis for the reformulated optimization model as described above.

While it is possible to use the approach in [13] also for the second step, we prefer to base the reduction on a multistage distance between trees which generalizes the Wasserstein distance and was recently proposed and analyzed in [32]. The advantage of this approach lies in the fact that the multistage distance is able to account for the development of information over time in a proper way: While the Wasserstein distance evaluates the similarity between trees based on values and probabilities and uses only one relevant σ-algebra, the multistage distance uses values and probabilities as well, but also takes into account the whole filtrations represented by the respective tree structures by using all conditional probabilies as well. This is illustrated by figure 5.1: From the standpoint of the Wasserstein distance both "trees" are very similar, even if ε is small, while the multistage distance sees a big difference, because of the splitting in the right tree.

Consider two trees with paths $\xi^i, \tilde{\xi}^j$ and probabilities $Q_i, \tilde{Q}_j$, and a distance d between paths $d_{ij} = d(\xi^i, \tilde{\xi}^j)$. Define conditional probabilities $Q(m|m_-) = \frac{Q_m}{Q_{m_-}}$, $j \in i_+$ and let π denote a joint probability model, such that π_{ij} are the probabilities for node i in tree Q, ξ and node j in tree $\tilde{Q}, \tilde{\xi}$.

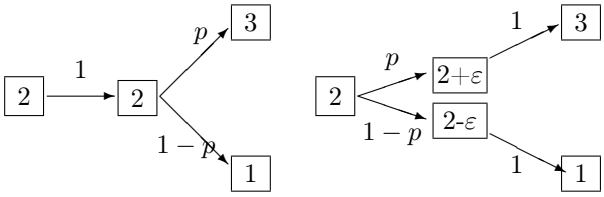

FIGURE 5.1. Two different flows of information. A distance that discriminates filtrations will make a big difference, even if $\varepsilon > 0$ is small

With

$$\pi(i,j|m,n) = \frac{\pi_{ij}}{\sum_{k\in m_+}\sum_{l\in n_+}\pi_{kl}}$$

the multistage distance $\mathsf{dl}_r(Q,\tilde{Q})$ is given as the optimal value of the following optimization problem

$$\begin{array}{ll} \text{minimize} & \sum_{i\in\mathcal{N}_T, j\in\tilde{\mathcal{N}}_T} \pi_{i,j}\cdot d^r_{i,j} \\ \text{(in } \pi\text{)} & \\ \text{subject to} & \sum_{j\in n_+}\pi\left(i,j|\,m,n\right) = Q\left(i|\,m\right) \quad (i\in m_+,\, n), \\ & \sum_{i\in m_+}\pi\left(i,j|\,m,n\right) = \tilde{Q}\left(j|\,n\right) \quad (j\in n_+,\, m), \\ & \pi_{i,j}\geq 0 \text{ and } \sum_{i,j}\pi_{i,j} = 1. \end{array} \tag{5.3}$$

In the tree approximation problem Q,ξ represent the big tree, while probabilities $\tilde{Q}$ and values $\tilde{\xi}$ of the smaller tree have to be chosen such that the distance dl is minimized. For this 5.3 is extended such that $\tilde{Q}$ (resp. $\tilde{Q}\left(j|\,n\right)$) are introduced as additional decision variables. While the original problem 5.3 can be reformulated as an LP, the extended approximation problem is nonconvex.

Therefore the extension of (5.3) is hard to solve exactly especially for large instances. [24] propose an algorithm that iterates between minimizing probabilities $\tilde{P}$ with given values $\tilde{\xi}$ and minimizing the values $\tilde{\xi}$ with given probabilities $\tilde{P}$. When improving $\tilde{P}$ a stagewise decomposition of the extended (5.3) with fixed $\tilde{\xi}$ is used. If the Euclidean distance is used as the basic distance d, improved values $\tilde{\xi}$ can be calculated in very fast manner as conditional means

$$\tilde{\xi}\left(n_t\right) := \sum_{m_t\in\mathcal{N}_t}\frac{\pi\left(m_t,n_t\right)}{\sum_{m_t\in\mathcal{N}_t}\pi\left(m_t,n_t\right)}\cdot\xi\left(m_t\right).$$

6. A numerical example and some results

In the following we apply the described optimization model to a concrete configuration of thermal power plants. The prices used for coal, gas and oil as well as for CO2 -certificates were simulated (and later on approximated by trees) from the price models analyzed in section 4. The implementation is used to consider two practical case studies: First we study the effects of increasing CO2 prices on the decisions made and second we analyze minimum production costs of electricity delivery contracts in the framework of indifference pricing.

FIGURE 6.1. *Simulated scenario paths for all used commodities.*

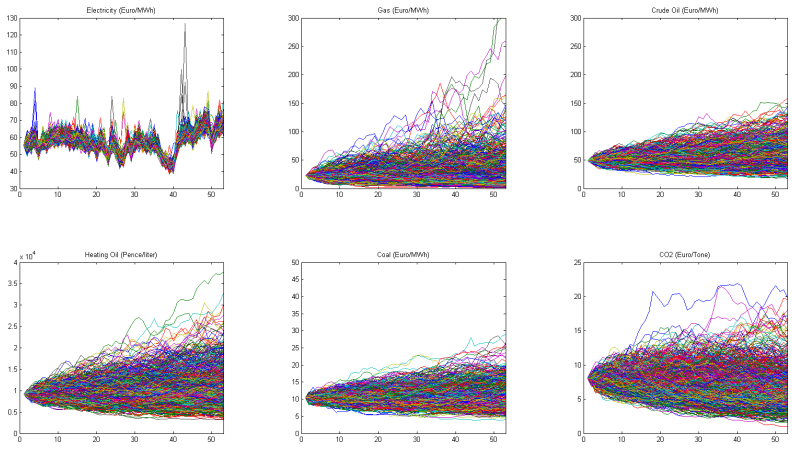

The thermal system consists of three combustion turbines, two combined cycle plants and one steam turbine. The steam turbine is fired with coal, whereas the other plants are able to use both gas or oil. The steam turbines are more efficient than the simple combustion turbines and the combined cycle plants are more efficient than the steam turbine. On the other hand, combustion turbines emit more CO2 than combined cycle turbines and steam turbines emit more CO2 than combustion turbines. The same order also holds for fixed and variable operating costs and for the size (maximum power) of the turbines. The exact numbers have been derived from typical engines described in [23] and can be found at http://homepage.univie.ac.at/raimund.kovacevic/publications.html.

Storage capacity is sufficient for approximately three weeks full production and the system starts with a small amount of stored fuel at the beginning. Again the related data, including storage costs, can be found at http://homepage.univie.ac.at/raimund.kovacevic/publications.html.

As described above we used historical data in order to estimate models for gas, oil, coal and electricity prices as well as CO2 emission prices. From the estimated models we simulate scenario paths for all commodities (see figure 6.1), calculate weekly averages, and finally construct a tree containing price and probability information. In particular we use a medium size tree with 52 stages representing the weeks of a year, 350 leaf nodes, representing the scenarios, and all in all 5950 nodes. The pure structure of the resulting tree is depicted in figure 6.2 and represents the filtration of the involved price and decision processes.

The cash position starts with a budget of 1 million EUR. In addition, interest on the cash position is given by 2.5% and interest on debt is 12.5%. Finally the average value at risk is calculated at level $\alpha = 0.05$. The mixture parameter λ is set to 0.5 in the standard case.

The model was implemented in AIMMS 3.12 and CPLEX 12.4 was used to solve all the instances discussed below. As a first result, figure 6.3 shows the development of the asset value v_t over time

while figure 6.4 shows an estimated p.d.f. of the asset value at the end of the planning horizon in more detail.

While we use the arbitrary value $\lambda = 0.5$ for the mixing parameter in the basic setup, it is possible to calculate an efficient frontier for the trade-off between expected end value and risk by calculating optimal solutions, while varying λ between zero and one. The results are shown in figure 6.5: For given risk, $\mathbb{E}(v_T) - AV@R(v_T)$, the points on the line show the largest expected end value possible - which is related to a certain value of λ.

6.1. **Varying CO2 emission prices.** For political reasons European CO2 emission prices are low at the time being and do not substantially reduce CO2 emissions. The basic model is now used to implement a simple analysis of the effect of CO2 prices on the optimal decisions. It should be

FIGURE 6.2. *Tree structure representing the filtration of the approximating processes used for numerical examples*

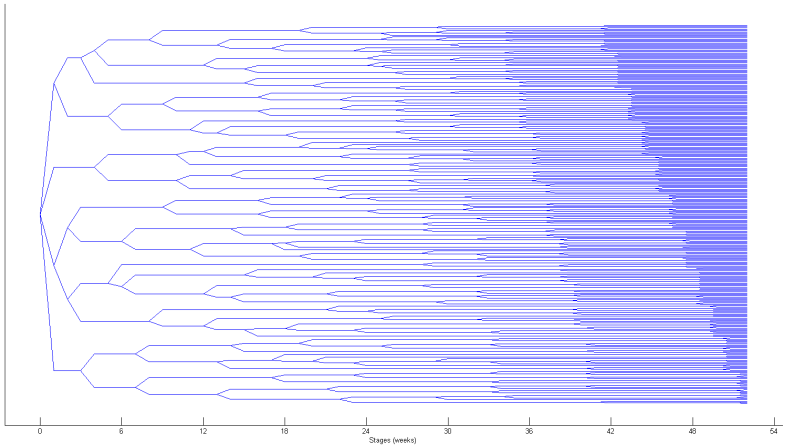

FIGURE 6.3. *Standard case: Development of the cash position over time*

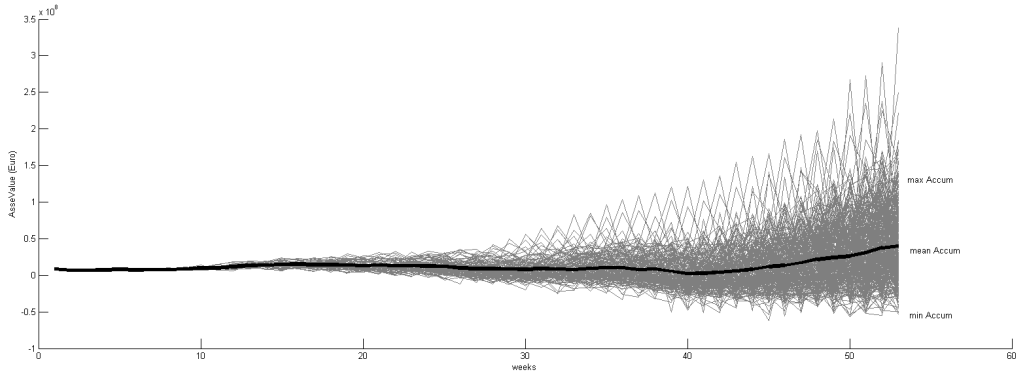

FIGURE 6.4. *Standard case: Distribution (distribution function) of the cash position at the end of the planning horizon*

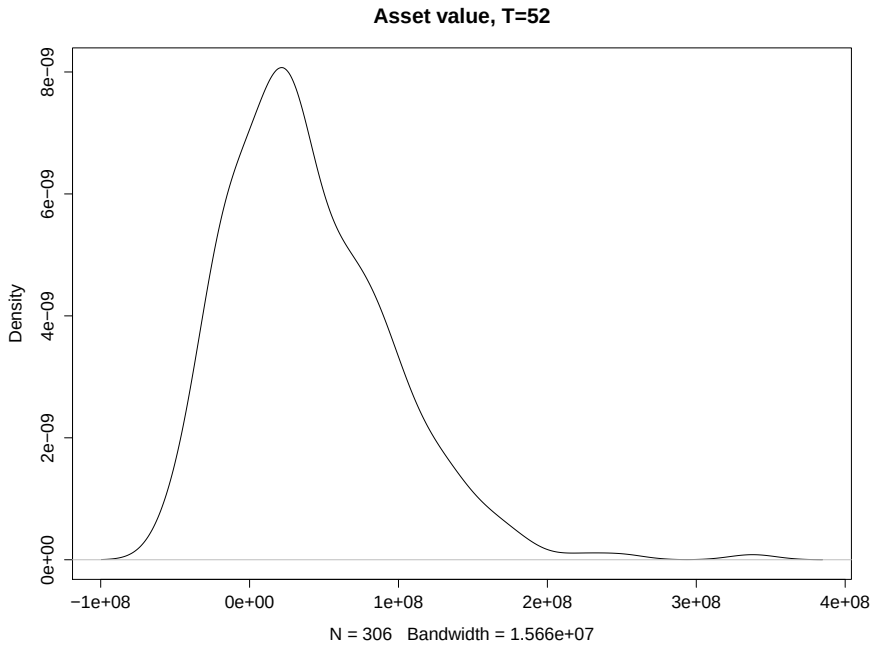

FIGURE 6.5. *Efficient frontier for the tradeoff between expected end value* $\mathbb{E}[v_T]$ *and riskiness* $\mathbb{E}[v_T] - AV@R_\alpha(v_T)$ *of the end value*

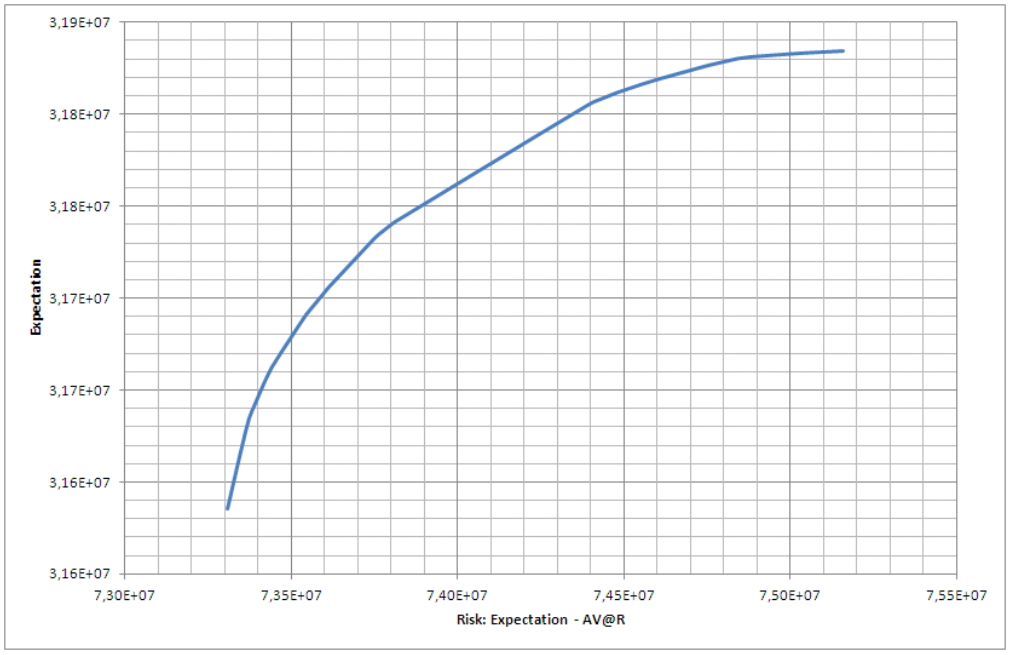

FIGURE 6.6. *Effect of an increase in CO2 prices on the accumulated CO2 emissions. The distribution of emissions is represented by a kernel density estimate.*

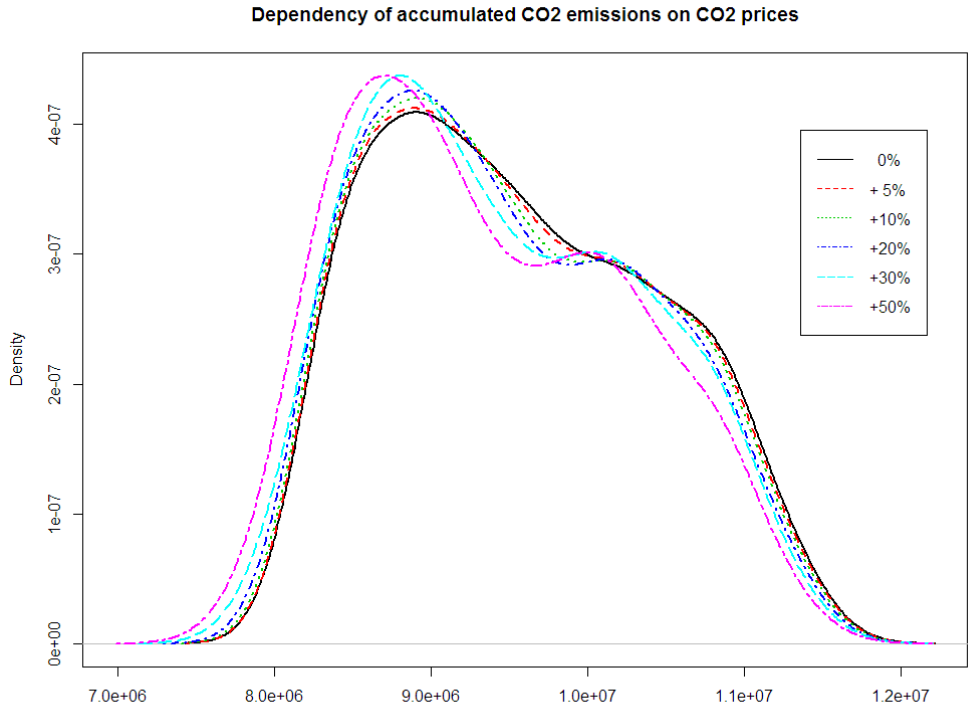

kept in mind that this is an analysis from the viewpoint of a producer with a certain given thermal system, not a market view.

The price scenarios are varied such that all CO2 prices are increased by $5\%, 10\%, 20\%, 30\%$ and 50%. For each of these scenarios problem 3.15 is solved to obtain the related optimal values and decisions.

Figure 6.6 depicts the effect of increasing prices on the amount of (accumulated) CO2, emitted over the whole planning horizon. Further results show that for the analyzed thermal system an overall increase of CO2 prices by 1% reduces the expected asset value by 1.66% but (on average) reduces the accumulated CO2 emissions by only 0.035%. The bimodal shape of the p.d.f. is mainly caused by the two types of gas/oil plants - if CO2 prices increase, production is gradually switched to the more efficient combined cycle plants. .

6.2. **Indifference pricing for electricity delivery contracts.** Assume now that additional to producing electricity for the spot spot market, one also considers electricity delivery contracts with given contract size in addition. For simplicity we consider contracts with a fixed (and constant) amount E of electricity deliverable during all weeks (52) of the planning horizon at a fixed, agreed price K per MWh. Hence, the generator has to produce some electricity and sell it at a fixed price,

regardless of the actual development of prices. Only excess production capacity can be used for trading at the spot market.

The question arises at which price – given our thermal system – the producer is willing to close a deal with given contract size. In the following we use indifference pricing as an approach to find this minimum price: The indifference principle states that the seller of a product compares his optimal decisions with and without the contract and then requests a price such that he is at least not worse off when closing the contract. This idea goes back to insurance mathematics ([6]) but has been used for pricing a wide diversity of financial contracts in recent years, see [7] for an overview.

To implement indifference pricing within our framework, problem 3.15 is solved to find the optimal value v^* without the analyzed contract. In a second step a modified optimization problem is formulated to find the minimal bid price: Because the producer should be indifferent, one constraint is given by

$$\lambda \cdot \mathbb{E}\left[v_T\right] + (1-\lambda) \cdot AV@R_\alpha(v_T) \geq v^*. \tag{6.1}$$

Next, it is allowed to buy electricity $y_t \geq 0$ at the spot market, and we ensure that the contract is fulfilled:

$$\sum_{i \in I, j \in J} x_{t,i,j} + y_t \geq E \tag{6.2}$$

Finally, the calculation of the cash position has to be corrected for the fact that parts of the electricity are sold at the contracted price K instead of the actual spot prices: (3.11).c is replaced by

$$P_t^x \cdot (\sum_{i=1}^{I} \sum_{j=1}^{J} x_{t-1,i,j} - E) + K \cdot E. \tag{6.3}$$

In order to find the indifference price we then solve the optimization problem

$$\begin{aligned} \min_{x,f,c,y,K,(s,w,v,a,e)} \quad & K \\ s.t. \quad & (3.1) - (3.13), \text{ using } (6.3) \\ & (6.1), (6.2) \qquad\qquad x, y, f, c \triangleleft \Sigma \\ & s, w, v, a, e \triangleleft \Sigma \qquad\qquad , \end{aligned} \tag{6.4}$$

Figure 6.7 shows the indifference prices for different contract sizes. It can be seen that the price is very high for small amounts of energy and decreases fast, due to effects of scale in production. For large contract sizes the price increases again, because for those amounts it is necessary to buy more and more electricity and to bear the resulting price risk.

The indifference approach can easily be modified for pricing forward contracts as contracts with delivery during some (future) part of the planning horizon. In the same way it is possible to analyze fuel contracts: In this case the producer seeks for the maximum price he is willing to pay for a fixed

FIGURE 6.7. *Indifference prices for varying contract size.*

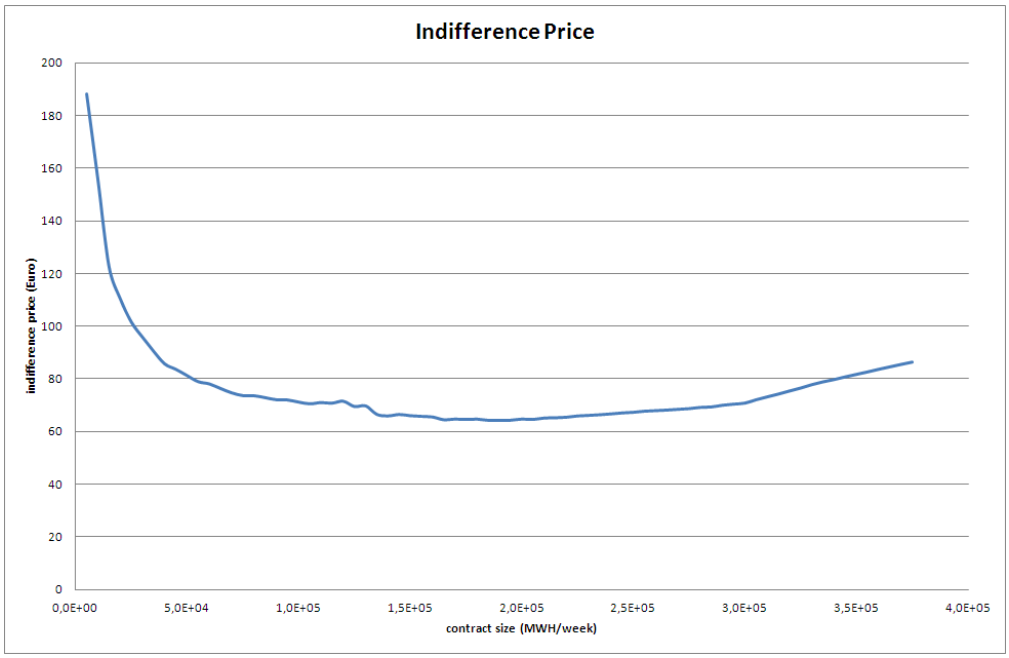

amount of fuel delivered during some specified period, such that he is indifferent with respect to the objective value.

7. CONCLUSIONS

In this paper we described a multistage stochastic optimization model for a thermal electricity production system with different types of fuels, the related random spot prices, fuel storage and CO2 emission certificates. In addition, costs involve fixed and variable operating costs. We maximize a mixture of expectation and average value at risk and derive the distribution of the asset value (a cash position plus the value of the fuel) at the end of the planning horizon. Going from data to some applications, several tasks had to be handled:

- We specified a flexible model for mid-term planning, such that iterative analysis – repeatedly using the optimization model – can be done in reasonable time.
- Our risk factors were the fuel prices for oil, gas, coal and CO2 emission certificates prices which are modeled as geometric Brownian motions with jumps. We further estimated electricity spot prices based on the related forward curve and deviations between this curve and actual prices. All models show a good in- and out of sample performance and they can be used for a realistic simulation of the future evolution of prices.
- Simulated hourly and daily commodity prices were aggregated to weekly average price scenarios and reduced to stochastic trees, suitable for stochastic multistage optimization.

- A concrete instance of the multistage optimization model – modeling weekly decisions over a full year – was implemented with fictitious but reasonable data, and used for some case studies.
- We analyzed variations in the overall level of CO2 prices and their effects to the production.
- Furthermore we investigated the pricing of electricity delivery contracts with fixed amount and price in the framework of indifference pricing.

The implementation was developed in discussion with practitioners from Siemens AG Austria and we hope to develop further some aspects of this work in our future research. In particular we will work to enhance the tree construction. Furthermore we see indifference pricing as an important approach at energy markets (applicable to all kinds of delivery contracts and forward contracts) and will try to understand deeper its theoretical and practical properties and implications.

Appendix A. Derivation of the shape

The derivation of the shape follows the procedure described in [5]. In a first step, we identify the seasonal structure during a year with working daily prices. In the second step, the patterns during a day are analyzed using hourly prices. Let us define two factors, the factor-to-year ($f2y$) and the factor-to-day ($f2d$). By $f2y$ we denote the relative weight of a single daily price compared to the annual base of the corresponding year:

$$f2y_d = \frac{S^{day}(d)}{\sum_{k \epsilon \text{year}(d)} S^{day}(k) \frac{1}{K(d)}} \tag{A.1}$$

$S^{day}(d)$ is the daily spot price in the day d, which is the average price of the hourly electricity prices in that day. $K(d)$ denotes the number of days in the year when $S^{day}(d)$ is observed. The denominator is thus the annual base of the year in which $S(d)$ is observed.

To explain the $f2y$, we use a multiple regression model (similar to [5]):

$$f2y_d = a_0 + \sum_{i=1}^{6} b_i D_{di} + \sum_{i=1}^{12} c_i M_{di} + \sum_{i=1}^{3} d_i CDD_{di} + \sum_{i=1}^{3} e_i HDD_{di} + \varepsilon \tag{A.2}$$

- $f2y_d$: Factor to year, daily-base-price/yearly-base-price
- D_{di}: 6 daily dummy variables (for Mo-Sun)
- M_{di}: 12 monthly dummy variables (for Feb-Dec); August will be subdivided in two parts, due to summer vacation
- CDD_{di}: Cooling degree days for 3 different German cities
- HDD_{di}: Heating degree days for 3 different German cities

where CDD_i/HDD_i are estimated based on the temperature in Berlin, Hannover and München.

- Cooling Degree Days (CDD) = $\max(T - 18.3°C, 0)$
- Heating Degree Days (HDD)= $\max(18.3°C - T, 0)$

We transform the series $f2y_d$ from daily to hourly, by considering the same factor-to-year $f2y_d$ for each hour t observed in the day d. This way we construct hourly $f2y_t$ series, which later enter the shape s_t. The $f2d$, in contrast, indicates the weight of the price of a particular hour compared to the daily base price.

$$f2d_t = \frac{S^{hour}(t)}{\sum_{k\epsilon \text{day}(t)} S^{hour}(k)\frac{1}{24}} \tag{A.3}$$

with $S^{hour}(t)$ being the hourly spot price at the hour t. We know that there are considerable differences both in the daily profiles of workdays, Saturdays and Sundays, but also between daily profiles during winter and summer season. Thus, following [5] we suggest to classify the days by weekdays and seasons and choose the classification scheme presented in table 1. The workdays of each month are collected in one class. Saturdays and Sundays are treated separately. In order to obtain still enough observations per class, the profiles for Saturday and Sunday are held constant during three months.

	J	F	M	A	M	J	J	A	S	O	N	D
Week day	1	2	3	4	5	6	7	8	9	10	11	12
Sat	13	13	14	14	14	15	15	15	16	16	16	13
Sun	17	17	18	18	18	19	19	19	20	20	20	17

TABLE 1. *The table indicates the assignment of each day to one out of the twenty profile classes. The daily pattern is held constant for the workdays Monday to Friday within a month, and for Saturday and Sunday, respectively, within three months.*

The regression model for each class is built quite similarly to the one for the yearly seasonality. For each profile class $c = 1, \ldots, 20$, a model of the following type is formulated:

$$f2d_t = a_o^c + \sum_{i=1}^{23} b_i^c H_{t,i} + \varepsilon_t \quad \text{for all } t\epsilon c. \tag{A.4}$$

where $H_i = 0, \ldots, 23$ represents dummy variables for the hours of one day.

The shape sw_t of the HPFC can be calculated by $sw_t = f2y_t \cdot f2d_t$. sw_t is the forecast of the relative hourly weights and it is additionally multiplied by the current yearly base product l[8]. This yields an hourly price forecast $s_t = sw_t \cdot l$, which is finally the shape which enters our objective function in 4.2.2.

APPENDIX B. ESTIMATION PROCEDURE FOR THE MERTON MODEL

The model parameters $\psi = (\alpha, \sigma, \lambda, \mu, \delta)$ in equation (4.1) are estimated by maximum likelihood. Prices S_t are observed at equally spaced time points $t_i = i\Delta$ for $i = 0, \ldots, T$, where Δ is the sampling

[8]For the horizon of one year we take the monthly and quarterly products and for the horizons longer than 1 year we take the yearly product to better reflect the particularities of the observed price forward curve.

frequency. For simplification, let S_i denote an observation of S at time t_i. The density function of the log return $x_{i+1} = \log S_{i+1} - \log S_i$ is

$$p(x;\psi) = \sum_{j=0}^{\infty} \frac{e^{-\lambda\Delta}(\lambda\Delta)^j}{j!} \phi\left(x; (\alpha - \frac{1}{2}\sigma^2)\Delta + j\mu, \sigma^2\Delta + j\delta^2\right) \tag{B.1}$$

where $\phi(x; m, v)$ is the density function of the normal distribution for mean m and variance v. The density of the log returns is evaluated by an infinite sum as in the density function of the Poisson distribution. For practical reasons, it is approximated by the first 100 terms of the sum in the estimation. The log-likelihood function becomes

$$l(x_1, \ldots, x_T; \psi) = \sum_{i=1}^{T} \log p(x_i; \psi). \tag{B.2}$$

However, it has been pointed out by [20], based on considerations in [22], that the likelihood function (B.2) may become unbounded for some parametric specifications if it is maximized without further restrictions on the parameter space. As a solution, it is proposed to link the variance of the standard Brownian motion σ^2 and the variance of the jump diffusion amplitudes δ^2, i.e., to set $\delta^2 = m\sigma^2$ for a fixed positive $m \in M$, where M is a compact set on $\mathbb{R}^+$. Then, the new log-likelihood function

$$l_m(x_1, \ldots, x_T; \psi^*) = l(x_1, \ldots, x_T; (\alpha, \sigma, \lambda, \mu, \sqrt{m}\sigma)) \tag{B.3}$$

can be maximized with respect to the reduced parameter vector $\psi^* = (\alpha, \sigma, \lambda, \mu)$ for a fixed value of m. As argued in [20], $l_m(\cdot; \psi^*)$ is bounded in contrast to $l(\cdot; \psi)$. Finally, a consistent estimator ψ is obtained by choosing the value of m which maximizes $l_m(\cdot; \psi_m^*)$.

Appendix C. Estimation procedure for the electricity model

Observations are given at (hourly) time points $t = 1, \ldots, T$. Let $h(t) : t \to \{1, \ldots, H\}$ a function that maps to each time point t the index of the corresponding week hour ($H = 168$ is the number of hours per week). In a first step, the observations are assigned to different regimes. The values that separate the Gaussian from the lower or from the upper spike regime, respectively, for each time band $h' = 1, \ldots, H$ are set to $\alpha_{h'} := \alpha \cdot s_{h'}$ for some parameter $\alpha > 0$ that is unique for all hours. $s_{h'}$ is the estimated standard deviation of $r_t := \ln MCP_t - \ln f_t$ for all $t = 1, \ldots, T$ with $h(t) = h'$, i.e., before assigning the observations to different regimes, but taking into account only positive prices. Define for each hour $h' = 1, \ldots, H$ the sets

$$\begin{aligned}
\mathcal{D}^L(h') &:= \{t = 1, \ldots, T \,|\, h(t) = h' \wedge MCP_t < f_t \cdot e^{-\alpha_{h'}}\} \\
\mathcal{D}^U(h') &:= \{t = 1, \ldots, T \,|\, h(t) = h' \wedge MCP_t > f_t \cdot e^{\alpha_{h'}}\} \\
\mathcal{D}^G(h') &:= \{t = 1, \ldots, T \,|\, h(t) = h' \wedge f_t \cdot e^{-\alpha_{h'}} \leq MCP_t \leq f_t \cdot e^{\alpha_{h'}}\}
\end{aligned}$$

that contain the indices of the hours that belong to one of the three regimes. Then, for each $h' = 1, \ldots, H$ the parameters are found by

$$\lambda^-_{h'} = \frac{\#\text{elements in } \mathcal{D}^L(h')}{\sum_{t\in\mathcal{D}^L(h')}(f_t \cdot e^{-\alpha_{h'}} - MCP_t)}$$
$$\lambda^+_{h'} = \frac{\#\text{elements in } \mathcal{D}^U(h')}{\sum_{t\in\mathcal{D}^U(h')}(MCP_t - f_t \cdot e^{\alpha_{h'}})}$$
$$\sigma_{h'} = \frac{1}{\#\text{elements in } \mathcal{D}^G(h')} \sum_{t\in\mathcal{D}^G(h')} (\ln MCP_t - \ln f_t)^2.$$

The value of α is chosen so that the log-likelihood function

$$\begin{aligned}\ln \mathcal{L}(\sigma_1, \ldots, \sigma_H, \lambda^+_1, \ldots, \lambda^+_H, \lambda^-_1, \ldots, \lambda^-_H \,|\, \alpha) = \\ \sum_{h'=1}^{H} \sum_{t\in\mathcal{D}^L(h')} \ln \phi_{exp}(f_t \cdot e^{-\alpha \cdot s_{h(t)}} - MCP_t \,|\, \lambda^-_{h'}) \\ + \sum_{h'=1}^{H} \sum_{t\in\mathcal{D}^U(h')} \ln \phi_{exp}(MCP_t - f_t \cdot e^{\alpha \cdot s_{h(t)}} \,|\, \lambda^+_{h'}) \\ + \sum_{h'=1}^{H} \sum_{t\in\mathcal{D}^G(h')} \ln \phi_{norm}(\ln MCP_t - \ln f_t \,|\, 0, \sigma_{h'})\end{aligned}$$

is maximized, where

$$\phi_{exp}(x \,|\, \lambda) = \begin{cases} \lambda e^{-\lambda x}, & x \geq 0 \\ 0 & x < 0 \end{cases}$$
$$\phi_{norm}(x \,|\, \mu, \sigma) = \frac{1}{\sqrt{2\pi\sigma^2}} \exp\left\{ -\frac{1}{2} \left(\frac{x-\mu}{\sigma} \right)^2 \right\}$$

are the densities of the exponential and the normal distribution with parameters $\lambda > 0$ and $\mu = 0, \sigma > 0$, respectively.

Appendix D. Symbols used in the optimization model

	Unit	Description
Sets and indices		
$\mathcal{I} = \{1, \ldots, I\}$		Set of thermal units
$i \in \mathcal{I}$		thermal unit i
$\mathcal{J} = \{1, \ldots, J\}$		Set of fuels
$j \in \mathcal{J}$		fuel j
$\mathcal{T} = \{\tau_0, \ldots, \tau_T\}$		considered points in time
$t \in T$		
$\Delta_t = \tau_{t+1} - \tau_t$	h	Length of time intervals
$\mathcal{N} = \{0, \ldots, N\}$		Set of nodes in a stochastic tree with root 0
$n \in N$		node n
$\mathcal{N}_T \subseteq \mathcal{N}$		Set of leaf nodes (scenarios)
$\mathcal{N}_{\neg T} \subseteq \mathcal{N} \setminus \mathcal{N}_T$		Set of all nodes excluding the leaf nodes
$\mathcal{N}_{\neg 0}$		Set of all nodes excluding the root nod
decision variables		
$x_{t,i,j}$	MWh	electricity produced with by unit i with fuel j during period $[\tau_t, \tau_{t+1}]$
y_t	MWh	electricity bought from spot market during period $[\tau_t, \tau_{t+1}]$
$f_{t,j}$	MWh	fuel of type j bought at time τ_t
$c_t(\omega)$	*metric tons*	CO_2-certificates bought at time t
calculated variables		
$s_{t,j}$	MWh	stored amount of fuel j at time t
w_t	EUR	Cash position
v_t	EUR	Asset value
a_t	(metric) tons	CO_2 certificates bought up to time t
e_t	(metric) tons	amount of CO_2 emitted up to time t
random factors		
$P^f_{t,j}$	EUR/MWh	mean spot price of fuel j over period $[\tau_t, \tau_t + \Delta_t]$
P^x_t	EUR/MWh	mean electricity spot price over period $[\tau_t, \tau_t + \Delta_t]$
P^c_t	EUR/tonne	mean spot price for CO_2 certificates over period $[\tau_t, \tau_t + \Delta_t]$
parameters		
η_{ij}		efficiency of burning fuel j with generator i
ε_{ij}	t/MWh	amount of CO_2 emitted by unit i per MWh of fuel burnt
β_j	MWh	maximum power that can be produced by generator i
γ_i	EUR/h	variable operating costs of machine i when fuel j is used
κ_i	EUR/h	fixed operating costs of machine i
ς_j	EUR/MWh	Storage costs for fuel j
σ_j	MWh	Maximum storage for fuel j
ϑ	EUR/tonne	Penalty for excessive CO_2-emissions
λ		Mixing factor for the objective function
α		Parameter of the average value at risk, $AV@R_\alpha$

$$\max_{x,f,c,(s,w,v,a,e)} \lambda \cdot \sum_{n\in\mathcal{N}_T} Q_n v_n + (1-\lambda)\cdot q$$

subject to

$$q \le g - \frac{1}{\alpha}\sum_{n\in\mathcal{N}_T} Q_n z_n$$

$$n \in \mathcal{N}_T : \; v_n - g + z_n \ge 0$$

$$n \in \mathcal{N}_{\neg T} : \; \sum_{j=1}^{J} x_{n,i,j} \le \beta_i \cdot \Delta_n$$

$$n \in \mathcal{N}_{\neg 0} : \; s_{n,j} = s_{n_-,j} + f_{n,j} - \sum_{i=1}^{I} \frac{x_{n_-,i,j}}{\eta_{i,j}}$$

$$n \in \mathcal{N} : \; 0 \le s_{n,j} \le \bar{s}_j$$

$$n \in \mathcal{N}_{\neg T} : \; \sum_{i=1}^{I} \frac{x_{n,i,j}}{\eta_{i,j}} \le s_{n,j}$$

$$n \in \mathcal{N}_{\neg 0} : \; e_n = e_{n_-} + \sum_{j=1}^{J}\sum_{i=1}^{I} \frac{\varepsilon_{ij}}{\eta_{i,j}} \cdot x_{n_-,i,j}$$

$$n \in \mathcal{N}^b_{\neg 0} : \; a_n = a_{n_-} + c_n n \in \mathcal{N}_{\neg T} \cap \mathcal{N}_{\neg 0} : \; w_n = (1+\rho_l)w^+_{n_-} - (1+\rho_b)w^-_{n_-}$$
$$+ P^x_{n_-} \cdot \sum_{i=1}^{I}\sum_{j=1}^{J} x_{n_-,i,j} - \sum_{j=1}^{J} \zeta_j \frac{(s_{n,j} + s_{n_-,j})}{2}$$
$$- \sum_{i=1}^{I} \frac{\gamma_i}{\beta_i} \cdot \sum_{j=1}^{J} x_{n_-,i,j} - \kappa_i \cdot \Delta_{n_-}$$
$$- \sum_{i=1}^{I} \frac{\gamma_i}{\beta_i} \cdot \sum_{j=1}^{J} x_{n_-,i,j} - \kappa_i \cdot \Delta_{n_-}$$

$$n \in \mathcal{N}_T : \; w_n = (1+\rho_l)w^+_{n_-} - (1+\rho_b)w^-_{n_-}$$
$$+ P^x_{n_-} \cdot \sum_{i=1}^{I}\sum_{j=1}^{J} x_{n_-,i,j} - \sum_{j=1}^{J} \zeta_j \frac{(s_{n,j} - + s_{n_-,j})}{2}$$
$$- \sum_{i=1}^{I} \frac{\gamma_i}{\beta_i} \cdot \sum_{j=1}^{J} x_{n_-,i,j} - \kappa_i \cdot \Delta_{n_-}$$
$$- (\theta + P^c_n)(e_T - a_T)^+$$

$$n \in \mathcal{N} : \; w_n = w^+_n - w^-_n$$

$$n \in \mathcal{N}_T : \; v_n = w_n + \sum_{j=1}^{J} s_{n,j} \cdot P^f_{n,j} + (a_n - e_n)^+ \cdot P^c_n$$

$$n \in \mathcal{N}_{\neg T} : \; x_{n,i,j} \ge 0 \, , f_{n,j} \ge 0$$

$$n \in \mathcal{N}_{\neg 0} : \; a_n \ge 0, \; e_n \ge 0$$

$$n \in \mathcal{N}_T : \; z_n \ge 0$$

$$n \in \mathcal{N} : \; w^+_n \ge 0, \; w^-_n \ge 0$$

$$s_{0,j} = s^0_j, \; e_0 = e^0, \; a_0 = a^0$$

$$w_0 = w^0 - \sum_{j=1}^{J} P^f_{0,j} f_{0,j}$$

FIGURE D.1. Tree formulation of the optimization problem

	GAS		**OIL**		**EUA**		**Coal**	
	P	**LR**	**P**	**LR**	**P**	**LR**	**LR**	
Mean	19.366	0.001	70.226	0.001	14.513	-0.001	70.633	0.001
Median	21.225	0.000	68.345	0.001	14.140	0.000	67.940	0.002
Maximum	39.750	0.251	145.860	0.135	28.590	0.156	139.710	0.148
Minimum	7.000	-0.350	25.240	-0.113	5.950	-0.145	42.460	-0.216
Std. Dev.	5.857	0.050	27.274	0.022	4.690	0.027	21.032	0.041
Skewness	-0.285	-0.339	0.410	-0.067	0.838	-0.229	0.918	-0.573
Kurtosis	2.095	9.501	2.424	5.431	3.722	7.859	3.578	6.576
Jarque-Bera	60.471**	2258.719**	93.685**	553.361**	147.509**	1055.005**	50.625**	192.072**
Probability	0	0	0	0	0	0	0	0
Nr. observations	1270	1269	2242	2241	1064	1063	328	327
$\rho(1)$	0.985	-0.109	0.997	-0.033	0.994	0.033	0.987	0.151
$\rho(2)$	0.973	-0.008	0.995	0.013	0.989	-0.023	0.967	0.081
$\rho(3)$	0.961	-0.001	0.992	0.027	0.983	-0.046	0.946	-0.039
$\rho(4)$	0.948	-0.031	0.99	0.015	0.978	0.049	0.925	0.09
$\rho(5)$	0.936	0.048	0.987	-0.034	0.972	-0.042	0.903	0.021

TABLE 2. Descriptive statistics of gas, coal, oil and EUA spot prices (P) and logarithmic returns (LR). Note: Two (one) stars denote significance at the 1% (5%) level; $\rho(t)$ are autocorrelation coefficients at lag t.

Test	Null Hypothesis	**GAS**		**OIL**		**EUA**		**Coal**	
		C	TC	C	TC	C	TC	C	TC
ADF	Unit Root	-2.667	-2.646	-1.781	-2.273	-1.038	-1.727	-1.929	-1.692
PP	Unit Root	-2.458	-2.435	-1.778	-2.272	-1.051	-1.741	-1.993	-1.785
KPSS	Stationarity	0.633*	0.473**	4.015**	0.538**	1.918**	0.389**	0.420*	0.148*

TABLE 3. *Unit root test results for gas, coal, oil and EUA logarithmic spot prices.* Note: The results are presented in both versions: by considering a constant C or a trend and a constant (TC) in the test equation. Two (one) stars denote significance at the 1% (5%) level. ADF refers to Augmented Dickey-Fuller test, PP to the Philips-Peron test and KPSS to the Kwiatkowski-Phillips-Schmidt-Shin test. The lag structure of the ADF test is selected automatically on the basis of the Bayesian Information Criterion (BIC). For PP and KPSS tests the bandwidth parameter is selected according to the approach suggested by Newey and West (1994).

		Gas	**Electricity**	**CO2**	**Oil**
Correlation	Gas	1.000	0.097	0.094	0.044
	Electricity	0.097	1.000	-0.003	0.005
	CO2	0.094	-0.003	1.000	0.196
	Oil	0.044	0.005	0.196	1.000
Sig. (1-tailed)	Gas	0.002	0.002	0.093	
	Electricity	0.002		0.460	0.436
	CO2	0.002	0.460		0.000
	Oil	0.093	0.436	0.000	

TABLE 4. *PCA of commodity prices. Correlation matrix.*

Component	**Explained variation**		
	Eigenvalue	% of Variance	Cumulative %
1	1.243	31.077	31.077
2	1.067	26.675	57.752
3	0.896	22.408	80.160
4	0.794	19.840	100.000

TABLE 5. *PCA of commodity prices. Total variance explained.*

	Component			
	1	2	3	4
Gas	0.478	0.542	-0.650	0.234
Electricity	0.196	0.772	0.589	-0.135
CO2	0.723	-0.257	-0.056	-0.639
Oil	0.673	-0.334	0.351	0.559

TABLE 6. *PCA of commodity prices. Component matrix.*

	Component			
	1	2	3	4
Gas	0.020	0.998	0.049	0.046
Electricity	0.002	0.049	0.999	-0.003
CO2	0.098	0.046	-0.003	0.994
Oil	0.995	0.020	0.002	0.098

TABLE 7. *PCA of commodity prices. Rotated component matrix.*

	Sample	Parameter estimation					
		α	σ	λ	μ	δ	ML
Crude oil	01.05.2003-01.12.2011	0.325	0.259	80.373	-0.0017	0.027	-5314.05
(monthly)		(0.141)	(0.013)	(19.490)	(0.0017)		
	01.05.2003-01.12.2010	0.283	0.271	68.981	-0.0013	0.028	-4705.27
		(0.149)	(0.013)	(17.156)	(0.0020)		
Heating oil	01.05.2003-01.12.2011	0.218	0.245	99.953	-0.0005	0.028	-5405.37
(monthly)		(0.134)	(0.011)	(18.398)	(0.0013)		
	01.05.2003-01.12.2010	0.158	0.253	103.751	0.0000	0.028	-4781.89
		(0.149)	(0.013)	(20.784)	(0.0014)		
EUA	01.04.2008-01.12.2011	0.178	0.254	81.165	-0.0051	0.036	-2152.87
(monthly)		(0.202)	(0.016)	(18.070)	(0.0029)		
	01.04.2008-01.12.2010	0.327	0.268	78.921	-0.0057	0.036	-1595.28
		(0.246)	(0.020)	(21.967)	(0.0037)		
Gas	01.04.2007-01.12.2011	0.321	0.379	99.790	-0.0006	0.068	-2015.13
(monthly)		(0.281)	(0.019)	(14.135)	(0.0038)		
	01.04.2008-01.12.2010	0.316	0.423	105.479	0.0003	0.071	-1514.65
		(0.361)	(0.025)	(17.925)	(0.0045)		
Coal	09.12.2005-01.12.2011	0.308	0.170	21.749	-0.0082	0.053	-552.264
(weekly)		(0.117)	(0.020)	(7.506)	(0.0068)		
	09.12.2005-01.12.2010	0.437	0.172	25.860	-0.0098	0.052	-450.484
		(0.140)	(0.024)	(10.157)	(0.0071)		

TABLE 8. *ML Estimation results of the GMBJ model for oil, EUA, gas and coal spot prices. Standard errors are in paranthesis.*

Estimation sample	R^2	MAPE
01.09.2008-01.12.2011	0.559	0.168
01.09.2008-01.12.2010	0.572	0.157

TABLE 9. *Statistics over 1000 spot prices scenarios versus historical prices*

FIGURE D.2. *1000 oil scenarios quatiles with start in 01.12.2011 for 300 days horizon*

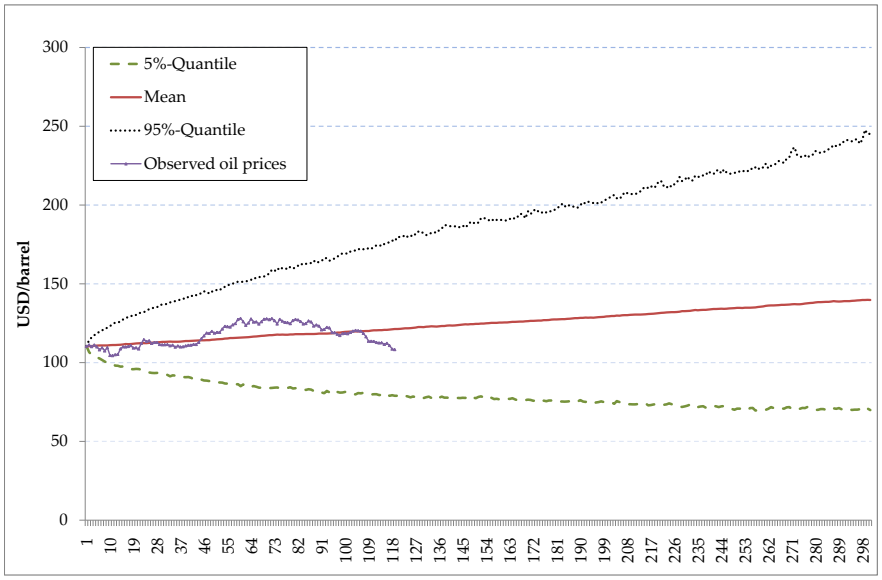

FIGURE D.3. *1000 EUA scenarios quatiles with start in 01.12.2011 for 300 days horizon*

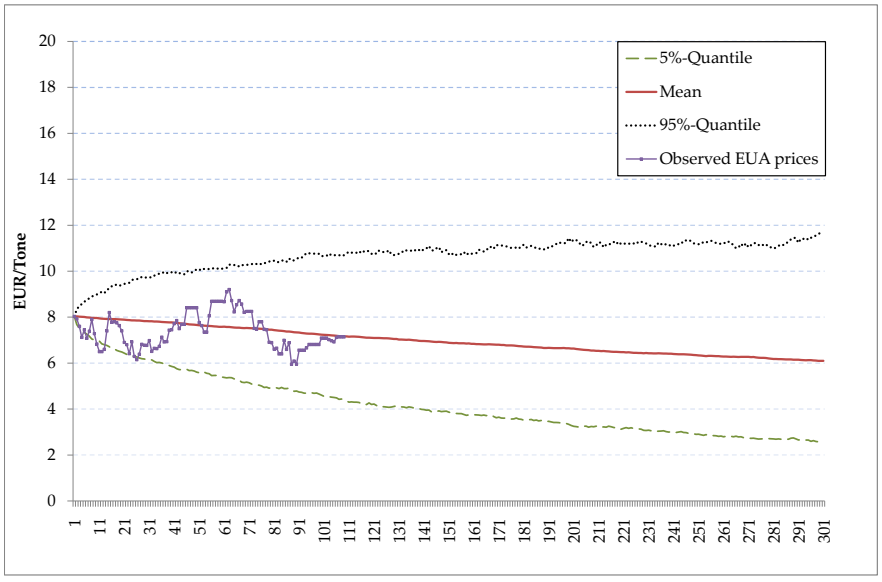

FIGURE D.4. *1000 gas scenarios quatiles with start in 01.12.2011 for 300 days horizon*

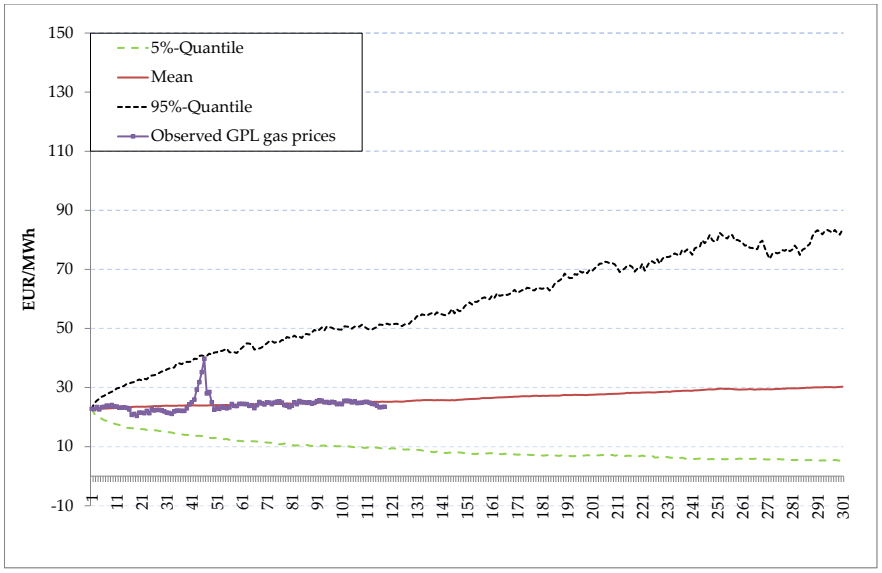

FIGURE D.5. *1000 coal scenarios quatiles with start in 01.12.2011 for 300 days horizon*

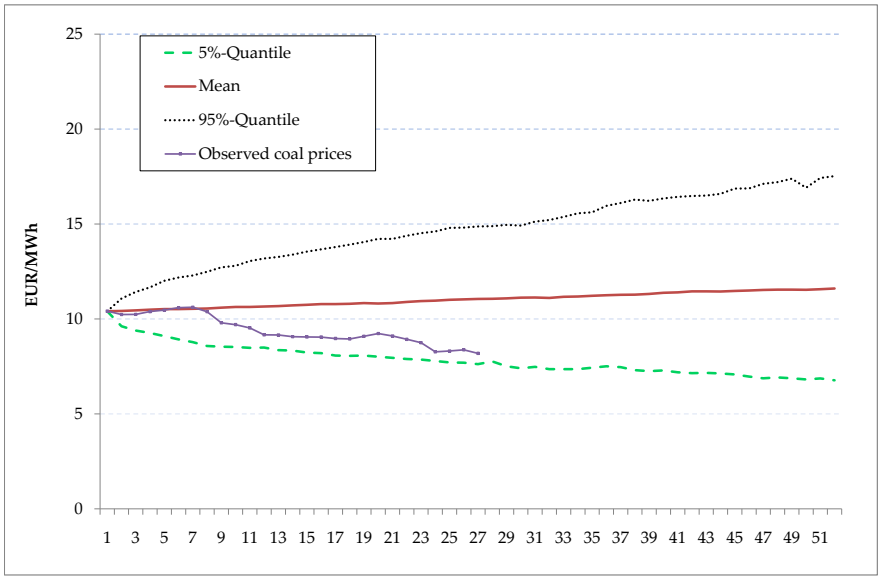

FIGURE D.6. *Occurrence of negative prices Sept. 2008-Dec. 2011 on different hours*

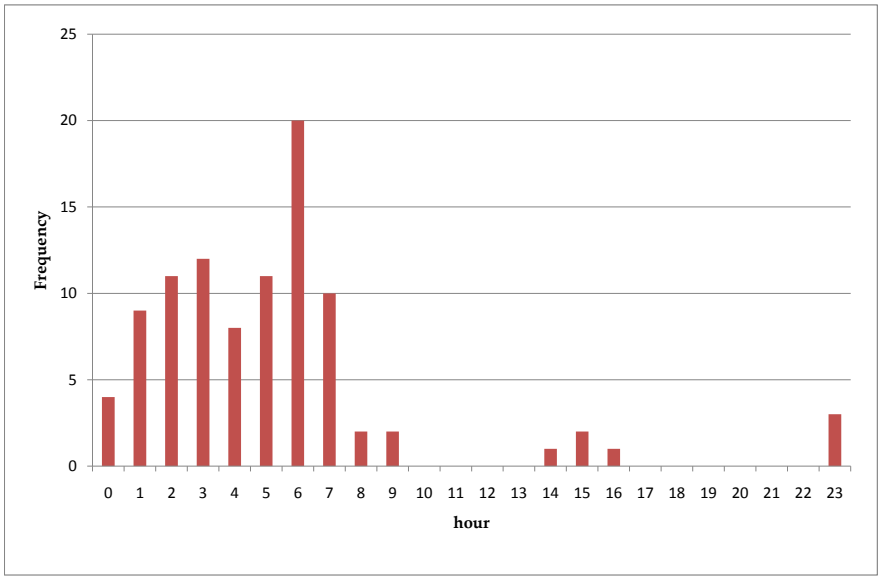

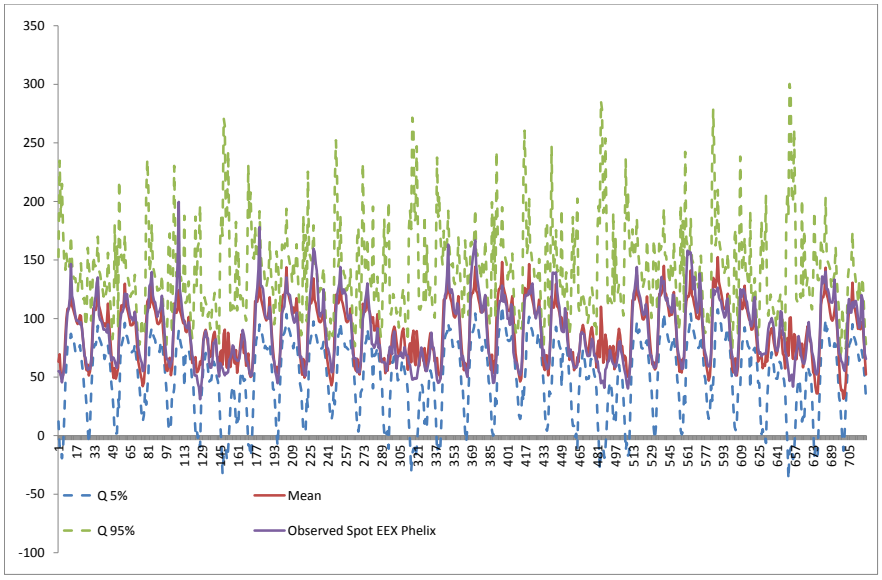

FIGURE D.7. *1000 EEX Phelix spot prices in sample scenarios quantiles starting in 01.09.2008 on a horizon of 1 month*

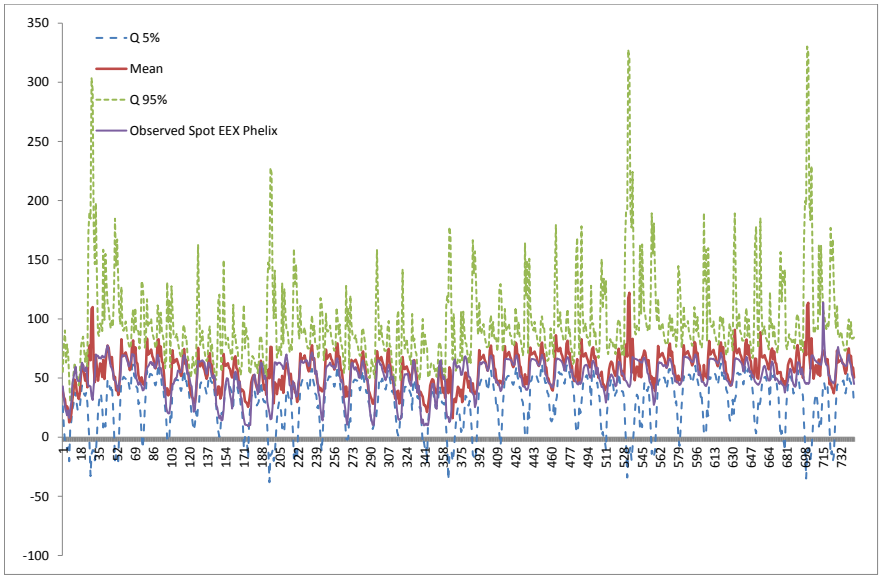

FIGURE D.8. *1000 EEX Phelix spot prices out of sample scenarios quantiles starting in 01.12.2011 on a horizon of 1 month*

$1/\lambda_h^+$	**23**	**24**	**1**	**2**	**3**	**4**	**5**	**6**	**7**	**8**
Mo	22.968	15.031	10.507	10.41	9.699	9.034	8.279	11.347	9.747	6.74
Tue	9.759	13.252	6.462	6.81	9.399	7.37	5.931	7.501	9.229	8.993
Wed	1.425	3.323	7.546	10.522	6.643	4.633	5.193	4.374	6.194	8.493
Thu		3.672	5.305	4.03	4.76	3.521	1.126	3.16	4.543	9.749
Friday	1.865	4.45		2.298	3.101	2.821	4.765	7.175	10.922	15.333
Sat	7.256	8.212	6.42	8.599	8.785	7.619	6.326	6.297	7.053	6.768
Sun	6.391	5.214	8.732	5.643	6.531	7.798	7.112	5.419	6.661	7.213
$1/(-\lambda_h^-)$	**23**	**24**	**1**	**2**	**3**	**4**	**5**	**6**	**7**	**8**
Mo	-5.55	-6.123	-9.334	-16.204	-12.309	-12.885	-13.394	-8.513	-7.871	-4.311
Tue	-9.455	-3.72	-2.889	-7.691	-12.892	-14.614	-7.855	-4.867	-8.388	-4.693
Wed	-9.077	-7.043	-7.673	-6.897	-10.703	-8.845	-7.368	-7.442	-22.79	-14.166
Thu			-2.12	-5.167	-5.136	-6.089	-5.095	-5.13	-12.701	-7.143
Friday		-17.454	-4.688	-7.946	-8.739	-7.05	-6.83	-4.563	-23.412	-6.556
Sat	-3.728	-23.612	-38.221	-34.27	-17.243	-15.134	-13.106	-11.639	-19.041	-50.885
Sun		-2.435	-5.529	-12.877	-28.122	-9.876	-7.973	-7.705	-10.351	-9.335
σ_h^2	**23**	**24**	**1**	**2**	**3**	**4**	**5**	**6**	**7**	**8**
Mo	6.88	5.958	6.135	6.244	6.403	5.925	6.229	6.478	7.835	10.209
Tue	6.624	6.079	4.847	5.489	5.625	6.119	6.047	5.75	6.422	10.604
Wed	5.908	4.879	5.504	5.658	5.889	5.616	5.357	5.405	6.417	10.769
Thu	5.831	4.348	5.882	5.756	5.96	6.258	6.049	4.724	5.671	10.386
Friday	5.803	4.893	5.396	5.481	5.428	5.304	5.461	5.261	5.501	10.335
Sat	6.289	5.823	4.794	5.15	4.725	5.509	5.908	5.421	5.929	6.234
Sun	6.656	6.052	6.203	5.103	5.34	5.068	4.264	4.687	3.739	4.24
p_h^+	**23**	**24**	**1**	**2**	**3**	**4**	**5**	**6**	**7**	**8**
Mo	1.77	3.54	4.425	5.31	6.195	7.965	7.965	2.655	5.31	4.425
Tue	2.655	2.655	3.54	5.31	6.195	9.735	9.735	3.54	5.31	2.655
Wed	0.885	0.885	0.885	1.77	3.54	7.965	6.195	0.885	1.77	0.885
Thu	0	0.885	0.885	2.655	2.655	5.31	3.54	0.885	4.425	1.77
Friday	1.77	3.54	0	2.655	7.08	9.735	7.08	3.54	6.195	2.655
Sat	3.54	3.54	3.54	2.655	3.54	4.425	5.31	4.425	7.965	5.31
Sun	11.504	12.389	11.504	21.239	22.124	23.894	23.894	24.779	24.779	23.894
p_h^-	**23**	**24**	**1**	**2**	**3**	**4**	**5**	**6**	**7**	**8**
Mo	0.885	3.54	20.354	25.664	34.513	39.823	35.398	20.354	3.54	7.965
Tue	0.885	3.54	7.965	11.504	14.159	18.584	18.584	7.08	0.885	3.54
Wed	0.885	1.77	3.54	10.619	11.504	15.929	15.929	6.195	1.77	3.54
Thu	0	0	1.77	5.31	11.504	14.159	9.735	5.31	3.54	4.425
Friday	0	2.655	1.77	3.54	7.08	10.619	7.965	5.31	4.425	3.54
Sat	1.77	1.77	3.54	4.425	10.619	12.389	15.929	19.469	15.929	4.425
Sun	0	4.425	7.965	15.929	23.009	30.973	32.743	36.283	42.478	27.434

TABLE 10. *Estimates of the regime-switching model for the night hours*

$1/\lambda_h^+$	**9**	**10**	**11**	**12**	**13**	**14**	**15**
Mo	4.319	3.452	5.313	81.671	33.664	0	0
Tue	9.798	9.493	12.096	14.018	1.031	5.746	0
Wed	9.377	6.01	5.635	9.255	0.512	3.646	0
Thu	5.526	1.021	4.811	12.62	4.3	2.829	1.913
Friday	9.041	3.689	1.181	11.062	4.556	1.126	0.403
Sat	3.94	3.899	4.253	1.571	3.914	4.726	2.441
Sun	5.875	7.171	7.367	8.937	7.55	9.714	6.877
$1/(-\lambda_h^-)$	**9**	**10**	**11**	**12**	**13**	**14**	**15**
Mo	-3.994	-3.492	-3.917	-2.231	-1.575	-1.485	-4.238
Tue	-6.42	-5.589	-6.203	-2.858	-3.169	-3.639	-2.96
Wed	-3.182	-1.258	-1.689	0	0	0	-0.536
Thu	-6.579	-1.99	-0.923	-1.395		-1.789	-0.815
Friday	-4.719	-6.549	-9.617	-4.34	-0.286	-2.638	-5.335
Sat	-38.794	-19.761	-6.676	-0.921	-1.478	-1.175	-7.156
Sun	-5.846	-4.762	-7.409	-4.587	-5.324	-7.451	-6.562
σ_h^2	**9**	**10**	**11**	**12**	**13**	**14**	**15**
Mo	9.13	8.989	8.93	10.167	9.165	8.82	8.143
Tue	10.723	10.946	9.839	10.318	8.637	8.335	8.093
Wed	10.623	11.535	10.137	11.443	10.323	9.88	9.83
Thu	9.162	8.591	8.66	10.631	8.619	8.267	8.277
Friday	8.663	8.589	9.013	9.67	8.177	7.78	7.668
Sat	5.838	6.307	6.451	6.949	7.169	6.4	5.393
Sun	5.002	5.312	5.597	5.81	6.483	6.385	5.815
p_h^+	**9**	**10**	**11**	**12**	**13**	**14**	**15**
Mo	1.77	0.885	1.77	0.885	0.885	0	0
Tue	1.77	1.77	1.77	1.77	0.885	0.885	0
Wed	2.655	1.77	1.77	1.77	1.77	0.885	0
Thu	1.77	0.885	2.655	3.54	2.655	1.77	0.885
Friday	1.77	0.885	1.77	1.77	0.885	1.77	0.885
Sat	3.54	1.77	0.885	0.885	0.885	0.885	2.655
Sun	22.124	10.619	8.85	7.08	7.965	5.31	9.735
p_h^-	**9**	**10**	**11**	**12**	**13**	**14**	**15**
Mo	3.54	2.655	3.54	6.195	1.77	1.77	3.54
Tue	2.655	2.655	1.77	1.77	1.77	1.77	2.655
Wed	1.77	0.885	0.885	0	0	0	0.885
Thu	2.655	1.77	0.885	0.885	0	0.885	0.885
Friday	1.77	0.885	0.885	0.885	0.885	1.77	2.655
Sat	3.54	2.655	2.655	0.885	0.885	2.655	1.77
Sun	13.274	7.08	2.655	3.54	2.655	6.195	7.08

TABLE 11. (a) *Estimates of the regime-switching model for the day hours*

$1/\lambda_h^+$	**16**	**17**	**18**	**19**	**20**	**21**	**22**
Mo	0	0	9.39	49.756	55.066	16.289	20.02
Tue	0	0	108.808	49.593	6.199	12.786	8.424
Wed	3.397	0	25.292	8.222	39.668	19.207	0.31
Thu	4.965	2.968	15.388	31.012	5.122	2.616	0
Friday	2.156	1.69	0.674	0	3.211	0	1.023
Sat	4.056	6.51	6.215	4.407	3.829	6.006	5.787
Sun	6.578	6.461	8.071	5.738	5.825	5.823	6.666
$1/(-\lambda_h^-)$	**16**	**17**	**18**	**19**	**20**	**21**	**22**
Mo	-3.884	-3.945	-2.222	0	-2.33	-3.646	0
Tue	-3.992	-4.443	-10.627	0	-0.658	-4.546	-5.862
Wed	-4.399	-3.669	-2.091	-6.921	-6.943	-9.205	-12.505
Thu	-2.458	-0.537	0	0	0	-9.764	-6.959
Friday	-5.423	-3.546	-1.484	-3.687	-6.77	-4.309	-10.269
Sat	-8.807	-4.368	-4.272	0	-1.999	-2.15	0
Sun	-6.279	-4.601	-2.325	0	0	-0.397	0
σ_h^2	**16**	**17**	**18**	**19**	**20**	**21**	**22**
Mo	7.654	7.494	9.793	12.301	8.071	8.836	7.914
Tue	7.823	7.973	7.787	11.565	10.138	9.022	7.179
Wed	8.146	7.694	8.866	9.48	8.79	8.474	7.587
Thu	7.458	7.965	8.943	8.304	8.348	8.57	7.214
Friday	7.529	7.664	6.959	7.02	8.893	7.085	6.095
Sat	4.882	5.38	8.104	8.396	8.281	7.178	6.018
Sun	5.432	4.898	7.165	7.673	8.038	7.608	6.954
p_h^+ **16**	**17**	**18**	**19**	**20**	**21**	**22**	
Mo	0	0	0.885	1.77	1.77	2.655	1.77
Tue	0	0	2.655	0.885	0.885	1.77	2.655
Wed	0.885	0	1.77	0.885	1.77	0.885	0.885
Thu	1.77	0.885	1.77	2.655	0.885	0.885	0
Friday	1.77	1.77	0.885	0	0.885	0	0.885
Sat	2.655	3.54	4.425	2.655	4.425	4.425	3.54
Sun	11.504	11.504	9.735	11.504	12.389	12.389	10.619
p_h^-	**16**	**17**	**18**	**19**	**20**	**21**	**22**
Mo	5.31	2.655	1.77	0	0.885	1.77	0
Tue	2.655	1.77	0.885	0	0.885	3.54	1.77
Wed	1.77	1.77	0.885	0.885	0.885	1.77	0.885
Thu	2.655	1.77	0	0	0	0.885	0.885
Friday	2.655	3.54	3.54	3.54	0.885	4.425	0.885
Sat	0.885	1.77	0.885	0	1.77	1.77	0
Sun	11.504	15.929	5.31	0	0	0.885	0

TABLE 11. (b) *Estimates of the regime-switching model for the day hours*

References

[1] Ball, C. A. & W. N., Torous, *Bond price dynamics and options*, Journal of Financial and Quantitative Analysis (18), pp. 517–531, (1983).

[2] Ball, C.A. & W.N., Torous, *On jumps in common stock prices and their impact on call option pricing.*, Journal of Finance 40, pp. 155–173, (1985).

[3] Beckers, S., *A note on estimating the parameters of the diffusion-jump model of stock returns*, Journal of Financial and Quantitative Analysis 16(1), pp. 127–140, (1981).

[4] Bierbrauer, M., C. Menn, T.R., Svetlozar & S., Trück, *Spot and derivative pricing in the EEX power market*, Journal of Banking and Finance, pp. 3462–3485, (2007).

[5] Blöchlinger, L., *Power prices - a regime-switching spot/forward price model with Kim filter estimation*, Dissertation of the University of St. Gallen, No. 3442, (2008).

[6] Bühlmann, H. *Mathematical risk theory*, Die Grundlehren der mathematischen Wissenschaften, Band 172, Springer, New York, (1972).

[7] Carmona, R. *Indifference pricing: theory and applications*, Princeton series in financial engineering, Princeton University Press, Princeton, (2009).

[8] Carrion, M. & Arroya, J. M. *A computationally efficient mixed-integer linear formulation for the thermal unit commitment problem*, IEEE Transactions on Power Systems, 21 (3), pp. 1371 – 1378, (2006).

[9] Casassus, J., Liu, P. & Tang, K, *Long-term economic relationships and correlation strucure in commodity markets*, working paper, (2010).

[10] Daskalakis, G., D. Psychoyios & R. Markellos, *Modeling CO2 emission allowance prices and derivatives: Evidence from the European trading scheme*, Journal of Banking and Finance, (2009).

[11] de la Torre, S, & Arroyo, J. M. & Conejo, A. J. & Contreras, J., *Price Maker Self-Scheduling in a Pool-Based Electricity Market: A Mixed-Integer LP Approach*, IEEE Transactions on Power Systems, 17 (4), pp. 1037 – 1042, (2002).

[12] Dickey, D.A. & W.A., Fuller, *Distribution of the estimators for autoregressive time series with a unit root.* Journal of the American Statistical Association No. 74, pp. 427–431, (1979).

[13] Dupacova, J. & Gröwe-Kuska, N. & Römisch, W., *Scenario reduction in stochastic programming: An approach using probability metrics*, Mathematical Programming, Series A (95), pp. 493–511, (2003).

[14] Eichhorn, A. & Römisch, W. & Wegner, I., *Polyhedral risk measures in electricity portfolio optimization*, Proc. Appl. Math. Mech., (4), pp. 7–10, (2004).

[15] A. Eichhorn & W. Römisch. *Polyhedral risk measures in stochastic programming*, SIAM J. Optim. (16), pp. 69 – 95, (2005).

[16] Fleten, S. & J. Lemming, *Constructing forward price curves in electricity markets*, Energy Economics 25, pp. 409–424, (2003).

[17] Frost, D. A., *The dual jump diffusion model for security prices*, Ph. D. Thesis, Department of Electrical Engineering and Computer Science, Massachusetts Institute of Technology, (1993).

[18] Gollmer, R & Nowak, W & Römisch, W. &, Schultz, R. *Unit commitment in power generation, a basic model and some extensions*, Ann. Oper. res. 96, 167-189, (2000).

[19] Heitsch, H & Römisch, W. *Stability and scenario trees for multistage stochastic programs*, in: Infanger, G. (Ed), Stochastic Programming, International Series in Operations research & Management Science, vol. 150, 139-164,(2011).

[20] Honoré, P., *Pitfalls in estimating jump-diffusion models*, working paper no. 18, University of Aarhus, (1998).

[21] Keles, D, M. Genoese, D. Möst & W. Fichtner, *Comparison of extended mean-reversion and time series models for electricity spot price simulation considering negative prices*, Energy Economics, (2011).

[22] Kiefer, N. M., *Discrete parameter variation: efficient estimation of a switching regression model*, Econometrica, No. 46, pp. 427-434 (1978).

[23] P. Konstantin, *Praxisbuch Energiewirtschaft - Energieumwandlung, -transport und -beschaffung im liberalisierten Markt*, Springer, (2007).

[24] Kovacevic, R. & Pichler, A., *Stochastic trees - a process distance approach*, available at www.optimization-online.org, (2012).

[25] Kwiatkowski, D., Phillips, P.C.B., Schmidt, P. & Y., Shin, *Testing the null hypothesis of stationarity against the alternative of a unit root: How sure are we that economic time series have a unti root?* Journal of Econometrics, No. 54, pp. 159–178, (1992).

[26] Manoliu, M. & S. Tompaidis, *Energy futures prices: term structure models with Kalman Filter estimation*, Applied Mathematical Finance, 9 (1), pp. 21–43, (2002).

[27] Meade N., *Oil prices - Brownian motion or mean reversion? A study using a one year ahead density forecast criterion*, Energy Economics, pp. 1485–1498, (2010).

[28] Merton, R.C., *Option pricing when underlying stock returns are discontinuous*, Journal of Financial Economics 3, pp. 125–144, (1976).

[29] Miltersen, K., *Commodity price modeling that matches current observables : a new approach*, Book, ID 6b00ce90-6fcf-11db-81a9-000ea68e967b, University of Southern Denmark, (2002).

[30] Nowak, N. P. & Schultz, R. & Westphalen, M., *A stochastic integer programming model for incorporating day-ahead trading of electricity into hydro-thermal unit commitment* , Optim. Eng., 6, 163-176, (2005).

[31] Paschke, R. & Prokopczuk, M., *Integrating multiple commodities in a model of stochastic price dynamics*, The Journal of Energy Markets, pp. 47–82, Volume 2/Number 3, (Fall 2009).

[32] Pflug, G. C. and Pichler, A., *A distance for multistage stochastic optimization models*, SIAM Journal on Optimization, 22 (1), pp. 1–23, (2012).

[33] Pflug, G. & Römisch, W., *Modeling, Measuring and Managing Risk*, World Scientific, (2007).

[34] Phillips, P.C.B. & P., Perron, *Testing for a unit root in time series regression*, Biometrika, No. 75, pp. 335–346, (1988).

[35] Philpott, A. & Schultz, R., *Unit commitment in electricity pool markets*, Math. Program., 108,313-337, (2006).

[36] Pilz, K.F. & Scholgl, E., *A Hybrid Commodity and Interest Rate Market Model*, Research Paper 261, (2009).

[37] Rockafellar, R. & Uryasev, S., *Optimization of conditional value-at-risk*, Journal of Risk, 2:21 (2000).

[38] Schwartz E., *The stochastic behavior of commodity prices: implications for valuation and hedging*, The Journal of Finance, Vol. LII, No. 3, (1997).

[39] Sen, S. & Yu, L., *A stochastic programming approach to power portfolio optimization, Oper. Res., 54(1), 55-72, (2006)*, Ph. D. Thesis, Department of Electrical Engineering and Computer Science, Massachusetts Institute of Technology, (1993).

[40] Takriti, S. & Birge, J. & Long, E. *A stochastic model for the unit commitment problem*, IEEE Trans. Power Syst., 11, 1497-1508, (1996).

[41] Treeck, T., *The hedge effectiveness of european natural gas futures*, Dissertation no. 3729, University of St. Gallen, (2009).

[42] Wallace, S. W. & Fleten, S. E., *Stochastic programming models in energy*, in: Ruszcynski, A. & Shapiro, A. (eds.), Stochastic programming, handbooks in Operations Research and management Science, vol. 10, 637-677, Elsevie, Amsterdam, (2003).